CO2 REMOVE
research monitoring verification

Contract n° SES6 518350

CO_2REMOVE

Instrument type: Integrated Project

Priority name: Sustainable Energy Systems

Final project report

Chapter 8

Ketzin test site

Authors:

Cornelia Schmidt-Hattenberger*
GFZ German Research Centre for Geosciences, Potsdam (Germany)

Peter Frykman
GEUS Geological Survey of Denmark and Greenland, Copenhagen (Denmark)

Peer-reviewed in June 2012 by:

Axel Liebscher, GFZ Potsdam (Germany)
Anna Korre, Imperial College London (UK)
Allan Mathieson, BP Aberdeen (UK)
Christian Bernstone, Vattenfall R&D Stockholm (Sweden)

*) Corresponding author: conny@gfz-potsdam.de, phone: +49 (0)331 288 1552; fax: +49(0)331 288 1502

Table of Content

8 KETZIN 3
8.1 Site characterisation and operational history 3
8.1.1 Geological background 4
8.1.2 Site conditions, drilling and well completion, injection history 5
8.2 Monitoring concept 7
8.2.1 Multi-disciplinary monitoring concept 8
8.2.2 The role of data integration 9
8.3 Monitoring data acquisition 27
8.3.1 List of data types and resolution 27
8.3.2 Timing and quality 28
8.4 Performance assessment (PA) 30
8.4.1 Reservoir modelling and flow simulation studies 31
8.4.2 Dynamic modelling of injections and predictions 35
8.5 Verification: Integration of PA and monitoring 36
8.5.1 Comparison of predictions and monitoring observations 36
8.5.2 Evaluation of comparisons 38
8.6 Conclusions and Outlook 40

REFERENCES 41

8 Ketzin

8.1 Site characterisation and operational history

The Ketzin pilot site was initiated in 2004 as the first demonstration project for geological onshore CO_2 storage in Europe within the frame of the European Union's CO_2SINK project, and is operated by the site owner Verbundnetz Gas AG (VNG) under the entrepreneurship of the German Research Centre for Geosciences (GFZ). The pilot site is located about 25 km west of Berlin in the German federal state of Brandenburg (Figure 8.1), and has been developed to inject CO_2 into a geological formation in the northeast German Basin (NEGB). It demonstrates an example of physical trapping of CO_2 in an anticlinal structure below low-permeability cap-rock structure (CO_2SINK Project Team, 2005).

Since the official start of CO_2 injection in June 2008, over 56,000 tonnes of CO_2 (status December 2011) have been injected into an Upper Triassic saline aquifer reservoir at about 630 to 650 m depth. Until 2004, the Ketzin anticlinal structure had been used for natural gas storage at 250 - 400 m depth in Jurassic sandstones (Schilling *et al*., 2009) as schematically drawn in Figure 8.2.

The storage site near the town of Ketzin, close to the cities of Berlin and Potsdam, includes industrial land and well developed infrastructure, and is surrounded by farmland. The operation of the CO_2 underground storage is regulated under German law according to the legislation of mining from the state of Brandenburg (Schilling *et al*., 2009).

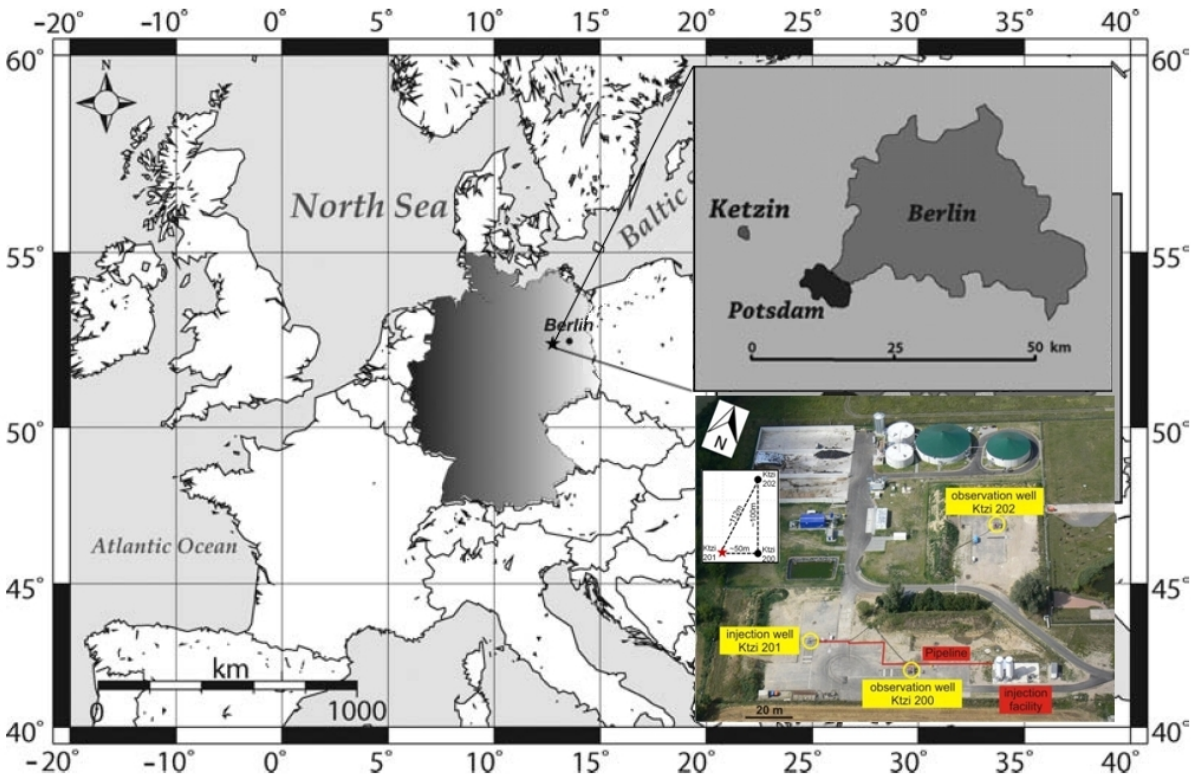

Figure 8.1 Location of the Ketzin site in Europe. Inset maps show details of the test site and its close vicinity to the cities of Berlin and Potsdam (modified after Kazemeini et al., 2009).

8.1.1 Geological background

The Ketzin-Roskow double anticline was formed by an elongated salt pillow situated at a depth of 1500 – 2000 m (Förster *et al*., 2006). The injection horizons are sandstones of the Upper Triassic (Keuper) Stuttgart Formation with variable thickness placed at depths of 630 to 650 m. The Stuttgart Formation is lithologically heterogeneous, consisting of sandy channel-facies rocks with good reservoir properties alternating with muddy flood plain facies rocks of poor reservoir quality (Förster *et al*., 2006; Norden *et al*., 2010). The upper seal of the Stuttgart Formation is the Weser Formation, consisting mainly of clayey and sandy siltstones, which alternate with carbonates and evaporites. The high clay mineral content and the observed pore-space geometry make these rocks a suitable seal for the CO_2 storage reservoir. The Weser Formation is overlain by mud/clay-carbonates of the Arnstadt Formation, which exhibits similar sealing properties (Förster *et al*., 2009).

Core Samples and NMR logs of the reservoir layer show permeabilities which integrate to aquifer permeabilities between 500 and 1100 mD (Norden *et al*., 2010). A minor part of the cores show cemented fissures with low permeability. However, pumping tests indicate aquifer permeabilities between 50 and 100 mD. The difference is interpreted to occur because the cemented fissures form a continuous structure. Since the distance between the fissures is typically larger than the core size, the representative elementary volume of the cores is too small and core permeability overestimates the aquifer permeability (Wiese *et al*., 2010).

The Ketzin storage complex is defined as follows: In vertical direction it covers the storage horizon which is the Stuttgart Formation and the secondary retention mechanism given by the caprock of the Weser and the Arnstadt Formation. The lateral extension is defined by the deepest, closed isobath of Top Stuttgart, which is the 710 m isobath of the Ketzin part of the Roskow-Ketzin anticline (Figure 8.2). The shallowest top seal is the Tertiary Rupelian claystone which acts as the uppermost barrier to movement of buoyant fluids at the site. It separates saline waters below from fresh and surface water above, but it does not belong to the Ketzin storage complex.

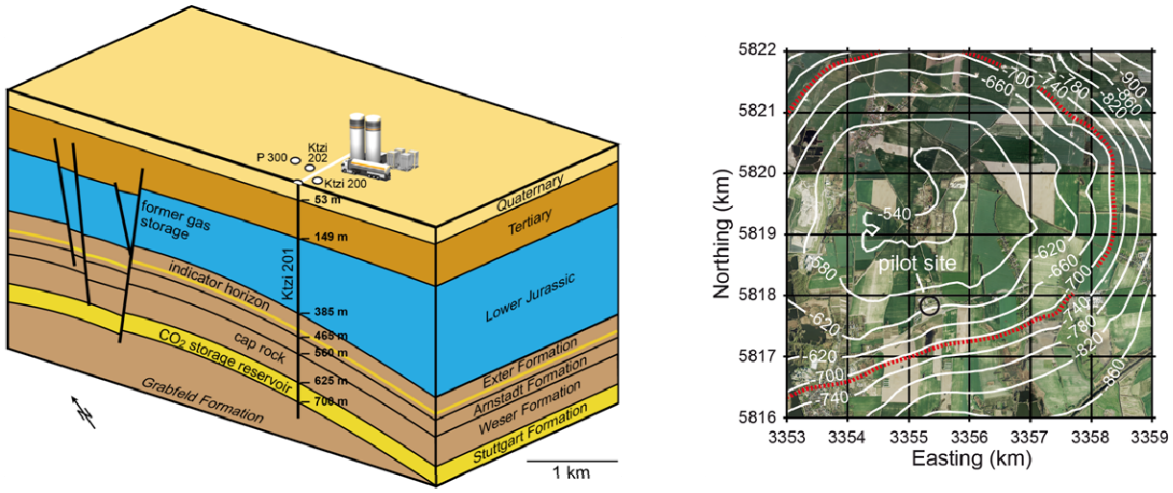

Figure 8.2 Schematic block diagram of the Ketzin storage site (left side, not to scale). In the Stuttgart formation, the target CO_2 storage zone covers the depth range 630 to 650 m. The 710 m isobathe defines the lateral extension of the Ketzin storage complex (right side). Figure re-drawn and modified after Liebscher et al. (2012).

8.1.2 Site conditions, drilling and well completion, injection history

Baseline 3D seismic data acquired in November 2005 confirmed the presence of an east-west trending Central graben fault zone (CGFZ). However, the southern part of the CGFZ is located more than 1.5 km north of the CO_2 injection site, and no faults could be detected in the seismic data in the vicinity of the pilot site (Juhlin *et al*., 2007). Remnant gas, cushion and residual gas, is present near the top of the anticline at the former gas storage in the depth interval of about 250–400 m and has a clear seismic signature (Kazemeini *et al*., 2007).
A ″gas chimney″, about 1 km long and 100 m wide, has been observed on the seismic data along the south-western main fault of the central graben fault zone (CGFZ). The gas chimney is a signature of leaking gas which has induced an amplitude brightening observed in a restricted volume along a fault zone. It is located above the upper gas layer, but below the base of the Tertiary, and is probably caused by gas migration from the Lower Jurassic formations into the fault zone at some stage during the gas storage operation. It is likely that either the reservoir pressure exceeded the fault reactivation pressure, causing the fault to move and therefore leak, or the reservoir pressure exceeded the fault capillary entry pressure (Juhlin *et al*. 2007).

Another typical characteristic of the site is the multi-barrier principle of the Ketzin storage site. A number of barriers are identified that can prevent the injected CO_2 from up-rising to the surface. These barriers are both engineered systems (wellbore cement and casing) and natural systems (caprock over the storage reservoir together with other low-permeability zones in the overburden), as described in detail in the Ketzin safety case of the long-term storage containment integrity (Flach et al., 2008). In this prototype risk assessment work, the concept of multiple geological barriers and the careful management of CO_2 injection volumes were key issues to meet the expected requirements of the CCS directive as well as to fit the demands for permission by the Mining authority of Brandenburg as local regulator.

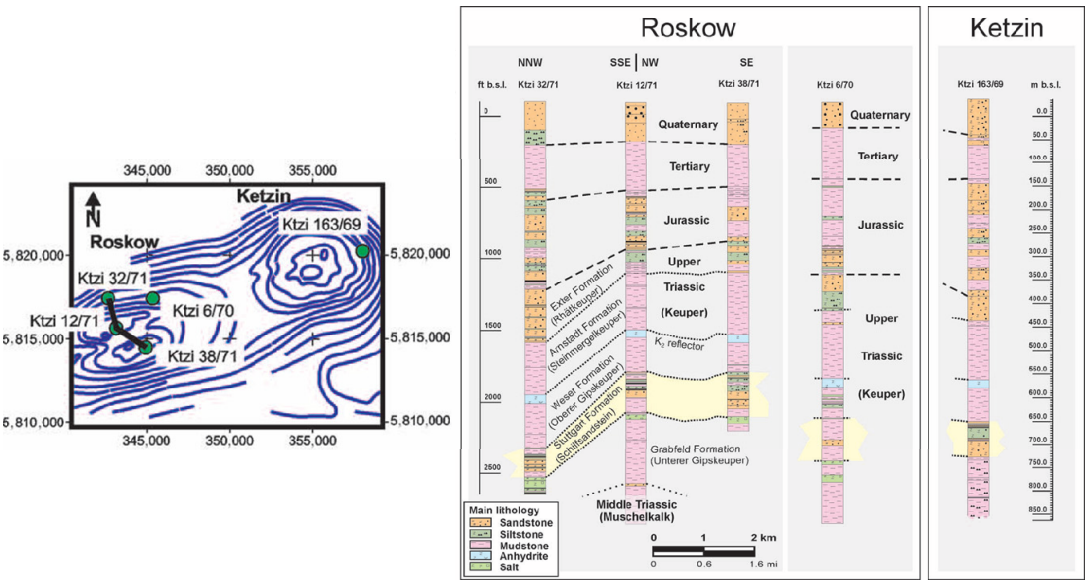

Figure 8.3 Stratigraphy of the Roskow-Ketzin double anticline (Förster et al., 2006). Cross-section through selected abandoned wells on the Roskow site west of the Ketzin anticline, including one abandoned well from the Ketzin anticline (Ktzi 163/69).

There is only one old well that penetrates the target storage reservoir on the Ketzin structure, well Ktzi 163/69, located more than 3 km away from the injection site and outside of the storage complex (Figure 8.3). There are over 40 old wells that penetrate the retired natural gas storage reservoir on the Ketzin structure, however. These have been sealed and abandoned applying a robust sealing solution that is technically feasible for a natural gas storage site. Although these wells are located within the storage complex, none of them are currently considered to be potential leak sources for the CO_2 storage project (Flach *et al.*, 2008).

One combined injection-observation well (Ktzi 201) and two observation wells (Ktzi 200 and Ktzi 202) were drilled into the southern flank of the Ketzin anticline in 2007, placed at the eastern part of the Roskow–Ketzin double anticline. All three wells were designed with the same casing layout, including stainless steel production casing equipped with pre-perforated sand filters in the reservoir section. The filter screens were selected to avoid unmanageable risk of potential damage for the variety of downhole cables as it could occur in case of standard in-situ perforation of the well pipe. These cables belong to the casing-conveyed monitoring sensors and covers two fibre-optical cable, a multi-conductor copper cable, and a Polyurethan-heating cable from the bottom of the casing to the surface. The reservoir casing section is externally coated with a fibre glass resin wrap for electrical insulation in order to deploy permanent downhole electrode arrays (Prevedel *et al.*, 2008). Adapted to the defined well completion a staged cementation program was performed.

Since 30th June 2008, food-grade quality CO_2 has been delivered by trucks from a chemical facility to the pilot site. The liquid CO_2 is stored in two 50 tonne-storage tanks, and from there alternately injected through the injection well Ktzi 201 (Figure 8.4). The CO_2 injection facility consists of five main plunger pumps (0–1000 kg h^{-1}), a heating device (305 kW_{el}) and two intermediate storage tanks (50 tonnes each). The facility was designed to handle a CO_2 stream of 300–3250 kg h^{-1} (200 kg h^{-1} stepwise) at 50 °C at the heater outlet, resulting in a maximum injection rate of 78 tonnes of CO_2 per day (Würdemann *et al.*, 2010).
During the CO_2SINK project an injected mass per day of about 56 tonnes up to 76.8 tonnes was achieved when the facility was in service, which corresponds to about 2.3 tonnes/hour up to about 3.2 tonnes/hour (Figure 8.5). In general, a continuous operating regime has been performed, where shut-in and re-start phases only occurred in case of scientific monitoring programmes (logging campaigns, crosswell seismic, deep fluid sampling etc.) and for necessary maintenance work.

Figure 8.4 CO_2 injection facility at Ketzin with the two intermediate storage tanks (left side), where the liquid, food-grade quality CO_2 delivered from chemical industry (right side) has been stored for the injection process (Photos: F. Möller, GFZ).

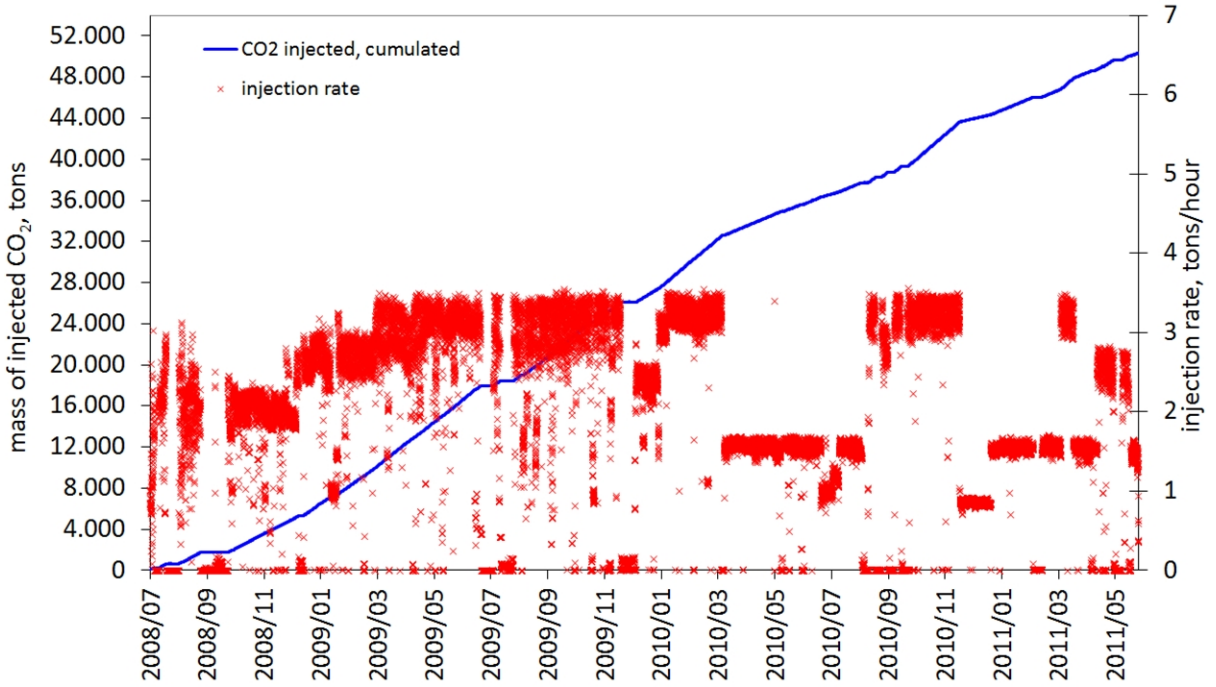

Figure 8.5 CO_2 injection history at Ketzin with a total of 48500 tonnes injected until May 1, 2011 (modified after Würdemann et al., 2010).

An automated control system monitors the injection process and its relevant parameters, as e.g. CO_2 flow, pressure and temperature at the well head. In the injection well Ktzi 201, pressure and temperature are additionally monitored with a fibre optic sensor at the end of the injection string. In addition, distributed temperature profiles have been recorded as real-time data along the injection string (see also paragraph 'Pressure and temperature measurement' below).

The control parameters were optimised during commissioning and four additional air-heaters were installed between the CO_2 pumps and the electrical heater to pre-heat the cooled and liquid CO_2 from -20 °C up to ambient conditions in order to reduce the required amount of electrical power for gas conditioning and to ensure a smooth injection regime.
The additionally installed air heaters reduced significantly the energy consumption (resulting in roughly 30 % energy saving, which corresponds to 50 kW) and smoothed out the measurable vibrations of the CO_2 column in the tubing during the injection process. All emergency shut-down (ESD) functionality is software independent and has been certified by the German testing organization **T**echnischer **Ü**berwachungs-**V**erein (TÜV) and the technical control board of the project. Furthermore, the mining authority approved the emergency and operation plans of the plant (Würdemann *et al*., 2010).

8.2 Monitoring concept

Ketzin was established as onshore CO_2 pilot site with the objective not to exceed the maximum allowed storage mass of about 100,000 tons of CO_2 in the saline aquifer, which defines the upper limit for a demonstration project. According the requirements for a basis of reliable data on the reservoir state during all operational phases one has to define sensitive and

robust monitoring technologies of high resolution to cover processes on different time and length scales. The measurements have to detect small differences of various quantities while the CO_2 migrates within the reservoir and interacts with the brine, the minerals and the borehole completions and casings. To achieve these goals, several disciplines as e.g. geophysics, geochemistry, and geomicrobiology have been applied from the surface as well as in the boreholes. For the wide range of deployed surface and downhole tools one has to assess their efficacy and usefulness. Due to the close spacing of the injection and monitoring wells as feature of this small-scale experiment the methods allow high resolution interrogation of the subsurface in the vicinity of the CO_2 plume (Figure 8.6).

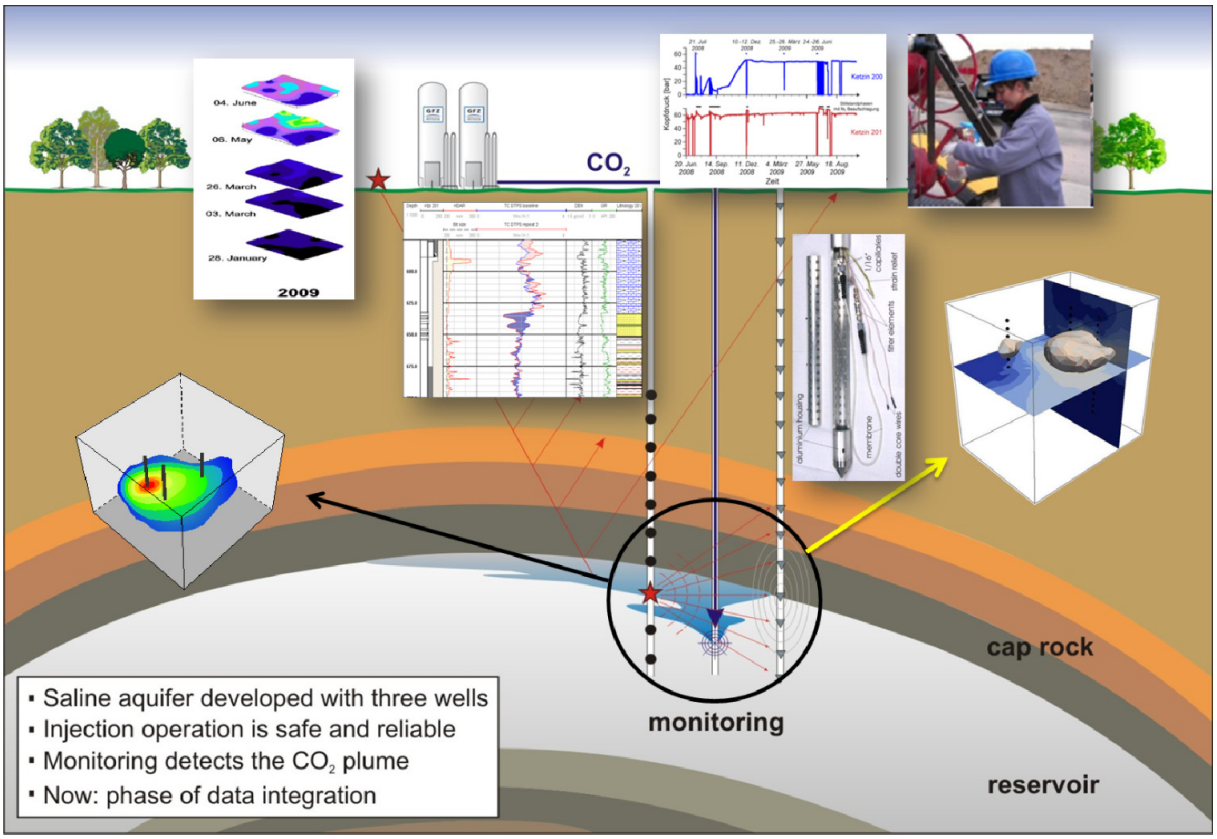

Figure 8.6 Types of monitoring deployed at Ketzin: seismic surveys, soil gas measurements, well logging, pressure-temperature measurements, gas membrane sensor for breakthrough detection, deep fluid sampling, and geoelectric surveys (from left to right, courtesy of GFZ).

The aim of this comprehensive monitoring programme is to demonstrate good understanding of plume migration in the subsurface and to demonstrate high detection capability of any potential leaks at the surface. Reliable data on the reservoir state during all operational phases yield the precondition for the comprehensive risk assessment framework which is the basis for safe and responsible geological CO_2 storage.

8.2.1 Multi-disciplinary monitoring concept

A very wide range of monitoring techniques is being tested at Ketzin. Their development and application was designed, developed and carried out in the frame of CCS research projects, as e.g. CO_2SINK, CO_2ReMoVe, COSMOS, COSMOS-2, CHEMKIN, COORETEC, etc., funded by the European Commission (Sixth Framework Program, FP6), two German

ministries - the Federal Ministry of Economics and Technology (COORETEC Program) and the Federal Ministry of Education and Research (GEOTECHNOLOGIEN Program) as well as many industry partners.

In this chapter, the Ketzin site will be considered in a holistic manner, regardless of the particular project-based origin of all individual research studies. This is in the spirit of the CO_2ReMoVe project, which focuses on the valuable experiences and findings from each of the international CO_2 storage test sites studied, and the subsequent contributions to guidelines and regulatory frameworks for CCS project operations in Europe in the near future.

8.2.2 The role of data integration

CO_2ReMoVe has contributed a relatively small but important subset of the total monitoring programme at Ketzin:

- MSP (3D VSP) (offset wellbore seismic)
- Distributed temperature sensor (DTS) along the injection tubing of well Ktzi 201
- Surface to wellbore electromagnetic surveys
- Passive seismic measurements (downhole and surface)

The above listed monitoring techniques supported the project objectives of tool optimisation and completion of the monitoring concept for the Ketzin test site. They provided an added value to the research in subproject SP 3 (site monitoring) and a direct contribution to subproject SP 2 (site performance) as well. In order to present an integrated picture and to point out the importance of data integration, results from many of the key surveys will be discussed here including the datasets acquired within CO_2ReMoVe. However, special emphasis will be put on the role of CO_2ReMoVe studies to address the issue of safe and reliable CO_2 storage operation by comparison of the site specific monitoring and verification frameworks elaborated in this project.

The monitoring technologies used at Ketzin include seismic and geoelectric surveys, wireline logs, tracers, and microbial and geochemical monitoring. All three wells are approximately 800 m deep and have permanent sensors cemented into the annular space behind the casing to monitor downhole pressure, temperature and electrical properties.

3D time-lapse surface seismic

The 3D surface seismic monitoring programme comprises baseline and repeat observations at different scales in time and space. 3D surface seismic baseline measurements, carried out in autumn of 2005 provide the structural model around the location of the injection and monitoring boreholes (Figure 8.7). The baseline survey covers 12 km^2, with a nominal 25-fold coverage (Juhlin *et al*., 2007). The main objectives of the seismic survey were to verify earlier geologic interpretations of the structure based on vintage 2D seismic and borehole data and to map the reservoir pathways in which the CO_2 is injected, as well as providing a baseline for future seismic surveys and planning of drilling operations. The uppermost 1000 m are well imaged and show an anticlinal structure with an east-west striking central graben at its top (Figure 8.7). No obvious faults were observed near the pilot site. Reservoir bodies to be 100-1000 m wide and 1-5 km long, and 5-30 m (3-20 ms) high are feasible to be detected within the resolution limit of the seismic data (Juhlin *et al*., 2007).

A spatial subset of the 3D baseline survey was repeated in autumn 2009, after around 23 k tonnes of CO_2 were injected, using the same acquisition geometry and hardware. The repeat survey was performed on an area covering around 50% of the baseline survey, concentrating on ~7 km^2 around the injection site and covering the maximum possible predicted propagation of the CO_2 in the reservoir. The most challenging task for onshore time-lapse seismic surveys is the implementation under reproducable operational as well as weather and grounding conditions. For the Ketzin 3D repeat survey a clear time-lapse effect of CO_2 injection has been analyzed. A defined amplitude-difference algorithm was applied based on baseline and repeat amplitudes for the horizon corresponding with top of Stuttgart Formation, and referred to the reference horizon of the so-called K2 reflector (Lüth *et al.*, 2011). The signal in the reservoir around the injection point is interpreted as indicating the extension of the free CO_2 plume (Figure 8.8). A first volumetric evaluation of the CO_2 plume has been carried out by comparing the 3D seismic repeat with gas saturation data from the pulsed neutron gamma (PNG) logging (Ivanova *et al.*, 2012).

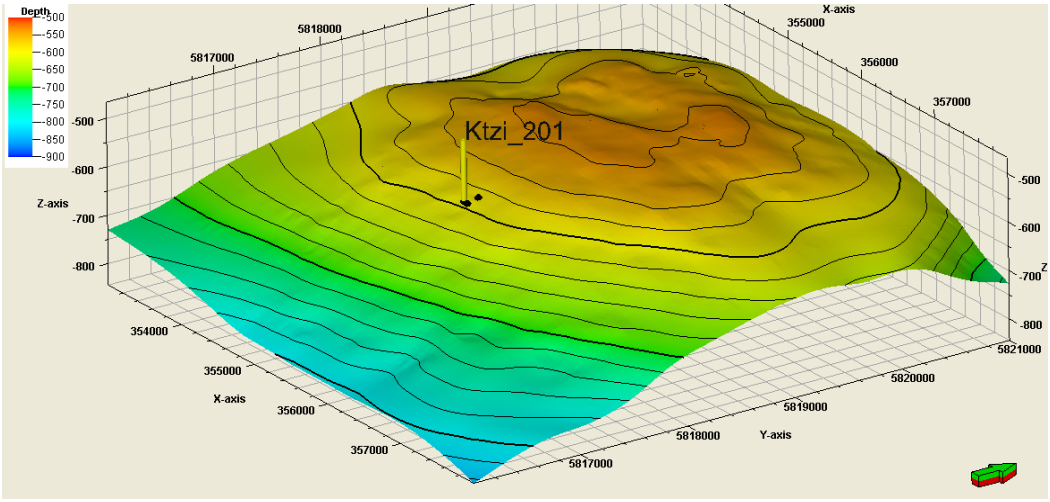

Figure 8.7 Map of the depth to top Stuttgart Formation interpreted from the 3D baseline seismic. The injection well Ktzi 201 is shown as well as position of the two observation wells (modified after Frykman, 2009a).

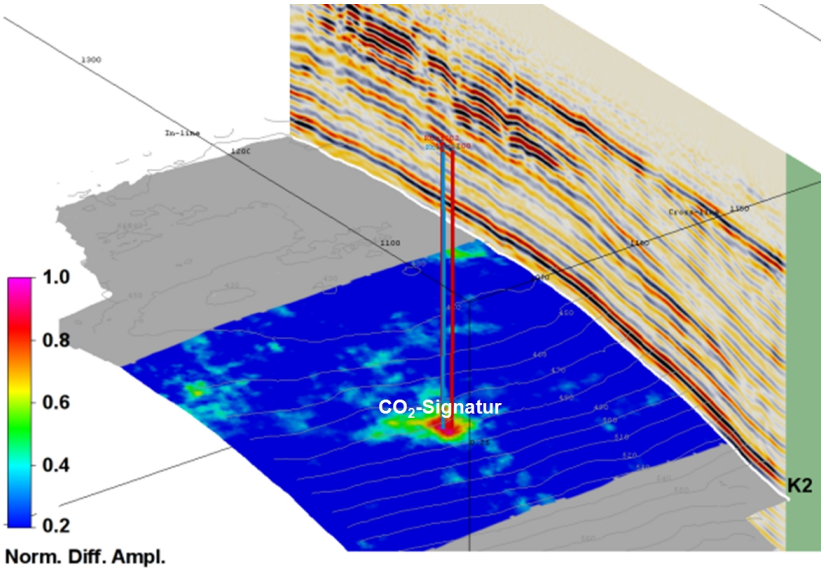

Figure 8.8 Repeat 3D seismic survey at Ketzin, showing vertical slice through the overburden and top reservoir slice showing amplitude differences around the injection point (Lüth et al., 2011).

2D time-lapse surface seismic

2D seismic lines were acquired in a 'star' configuration by baseline survey in 2005, by a first repeat survey in September 2009 (22-25 kilotons of CO_2 injected) and by a 2nd repeat survey in February 2011 (45 kilotons of CO_2 injected). For this star-like geometry, seven surface seismic shot/receiver lines (lines V1 to V7) and two shorter receiver lines (lines 19 and 20) perform a radial distribution of acquisition profiles directed towards the approximate location of the injection well (illustration see under Wellbore seismic, Figure 8.11). The data acquisition was operated in that mode providing a standard 2D survey for each line and for a focussed pseudo-3D survey near the wells (Ivandic et al., 2012). The obtained data potentially yield enhanced temporal and spatial resolution due to the higher source and receiver frequencies (Bergmann *et al*., 2011). A major objective consists in the evaluation of this star-like acquisition concept as cost-efficient alternative tool for plume tracking instead of the full 3D seismic repeat.

Wellbore seismics

The downhole seismic measurements acquired in different time-windows from 2008 – 2011 comprise baseline and repeat observations of zero-offset and offset Vertical Seismic Profiles (VSP), 2D and 3D MSP (moving source profiling) and crosshole tomography (Yang *et al*., 2010; Götz *et al*., 2011a; Cosma and Enescu, 2011).

While the 3D seismic survey provides data over a large area of several square kilometres but with relatively low spatial resolution, borehole seismic measurements focus on a smaller area around the measurement well with higher spatial resolution, in a figurative sense covering the region around the injection point. The gain of the resolution will be obtained by increased frequency, which is up to 2000 Hz for the crosshole measurement and up to 70 Hz for the VSP and MSP measurements. In the Ketzin case, the seismic rays are strongly bent within the K2 anhydrite layer. This limits the region covered around the injection site to a radius of ~300 m in the depth of the reservoir. The wellbore seismic is an add-on to the surface seismic, in case more detailed information is needed about the structure in the vicinity of borehole.

Three examples of the wellbore seismic measurements will be shown, illustrating the different scales of the measurements: The crosshole is measured between the wells, the zero-offset VSP is a surface-to-borehole measurement close to the well, whereas the offset VSP source points have distances of several 100 m to the well.

<u>Crosshole:</u>

Four crosshole measurements were performed: a baseline survey in May 2008, two repeats in July and September 2008, and a third one in July 2009. The observation wells Ktzi 200 and Ktzi 202 were used for sources and receivers, respectively. The results show no significant time-lapse effect in the first repeats, but the third repeat revealed a clear travel-time delay in the observations, indicating a velocity reduction in the reservoir as expected due to the expanding CO_2 plume (Cosma and Enescu, 2011, Lüth *et al*., 2011). Figure 8.9 shows the P-wave velocity model derived from travel time tomography of the crosshole data. The velocities are calculated on a plane between the observation wells. The wells are indicated as well tracks and the lithology within the wells is shown. Ktzi 200 is on the left side and Ktzi 202 is on the right side. The reservoir sandstone is marked with a star. The highest velocity of >5500 m/s is measured within the anhydrite layer (K2). Seismic rays are bent into the seismically fast layers, which are surrounded by zones of low ray coverage (white zones in Figure 8.9). The reservoir is characterised through a low velocity of <3000 m/s and a low ray coverage. The velocity model derived from the crosshole tomography of Figure 8.9 can be used for the depth migration of the VSP data (Figure 8.12

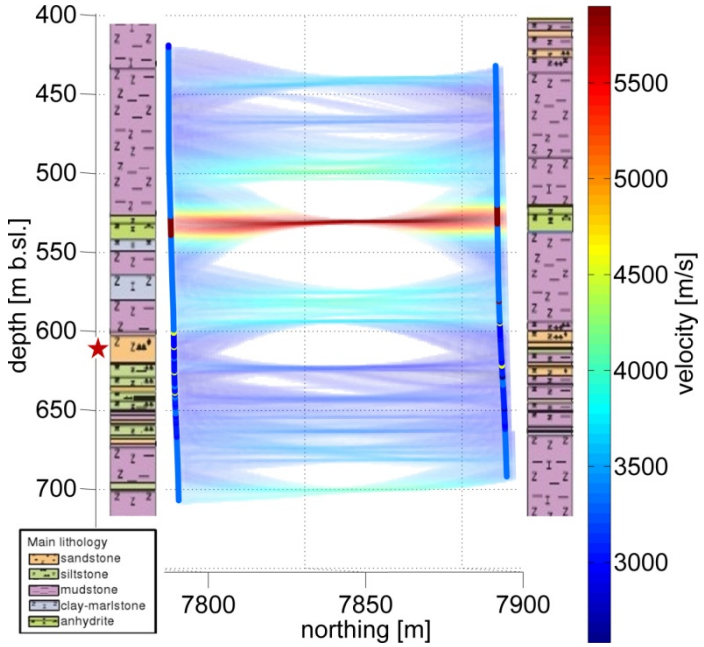

Figure 8.9 P-wave velocity model derived from travel time tomography of the crosshole data. The velocities are calculated on a plane between the observation wells. The wells are indicated as well tracks, and the lithology within the wells is shown. Ktzi 200 is on the left side and Ktzi 202 is on the right side. The reservoir sandstone is marked with a star. Figure re-drawn and modified after Götz, 2012.

Zero-offset VSP:

Prior to injection the zero-offset VSP baseline was measured in November/December 2007. The repeat of the zero-offset VSP was measured in February 2011 with 45,770 t CO_2 injected. The receivers were placed in the observation well Ktzi 202. Figure 8.10 shows the zero-offset VSP difference, repeat minus baseline, inserted into a slice of the 3D surface seismic difference crossing the injection well. The time-lapse amplitudes of the zero-offset VSP image the reservoir with a high resolution and can be compared to the time-lapse amplitudes of 3D surface seismic. The amplitudes show an increased reflectivity from the sandstone layers of the Stuttgart formation. The increased reflectivity is caused by a decreased P-wave velocity of the rock units affected by CO_2 injection.

Offset VSP:

The layout of the surface-to-borehole seismic measurements is summarized in Figure 8.11. The source points of the 2D MSP lie on 7 profiles around the injection site, the same locations as used for the 2D surface seismic measurements. For the offset VSP, the source is positioned at two locations, at the far end and in the middle of each of these 7 lines. The source points of the 3D MSP are the same as for the 3D surface seismic repeat. All surface-to-borehole seismic measurements are recorded in the observation well Ktzi 202.

Figure 8.12 shows offset VSP baseline data of the southern source point on line V1 of Figure 8.11, inserted for comparison into the 3D dataset at Ketzin. The distance between the source point and the receiver well is 606 m. The offset VSP data is in good correlation to the 3D surface data, with a more detailed structure in the deeper part of the section. These results are a promising baseline for a time-lapse analysis of the VSP data.

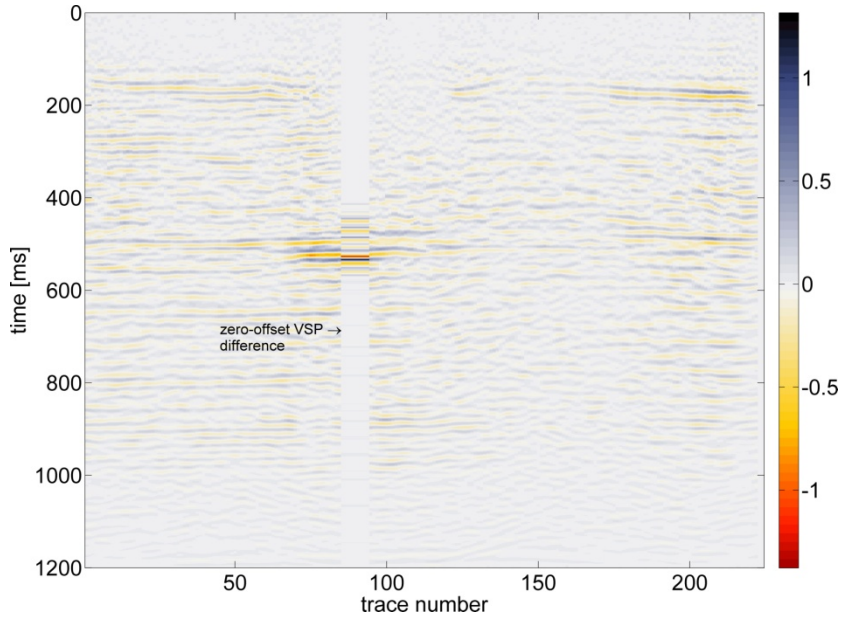

Figure 8.10 Zero-offset VSP difference, repeat minus baseline; inserted into a slice of the 3D surface seismic difference crossing the injection well. Figure re-drawn and modified after Götz, 2012.

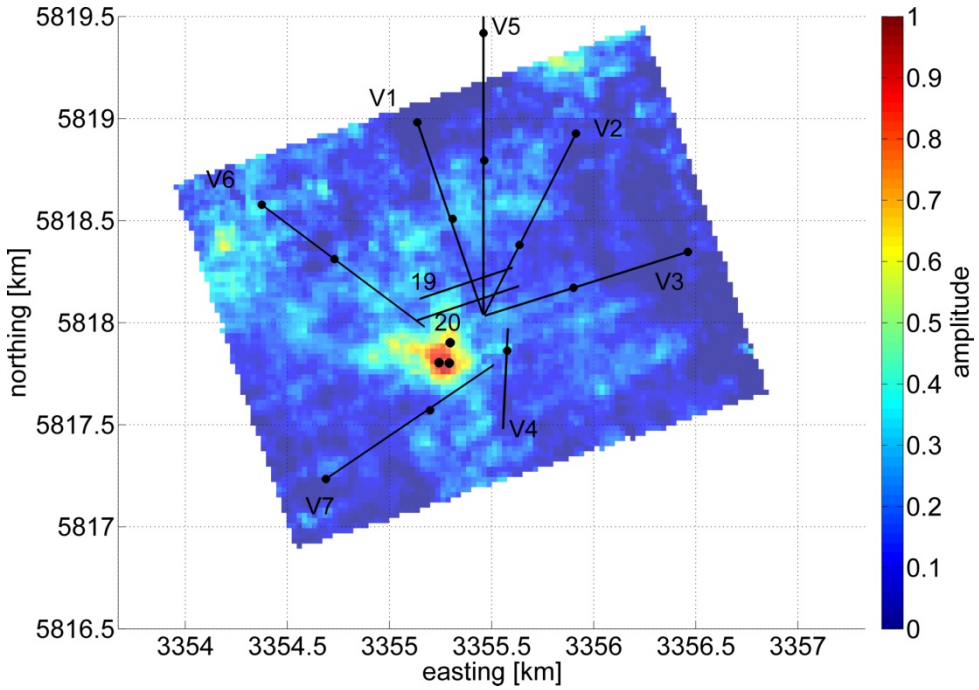

Figure 8.11 Layout of the wellbore seismic measurements plotted on top of the 3D surface seismic amplitude differences (Ivanova et al., 2012). The seven 2D MSP source lines are the same as used for the 2D time-lapse surface seismic. The dots on the lines indicate the position of the offset VSP source points. Figure re-drawn and modified after Götz, 2012.

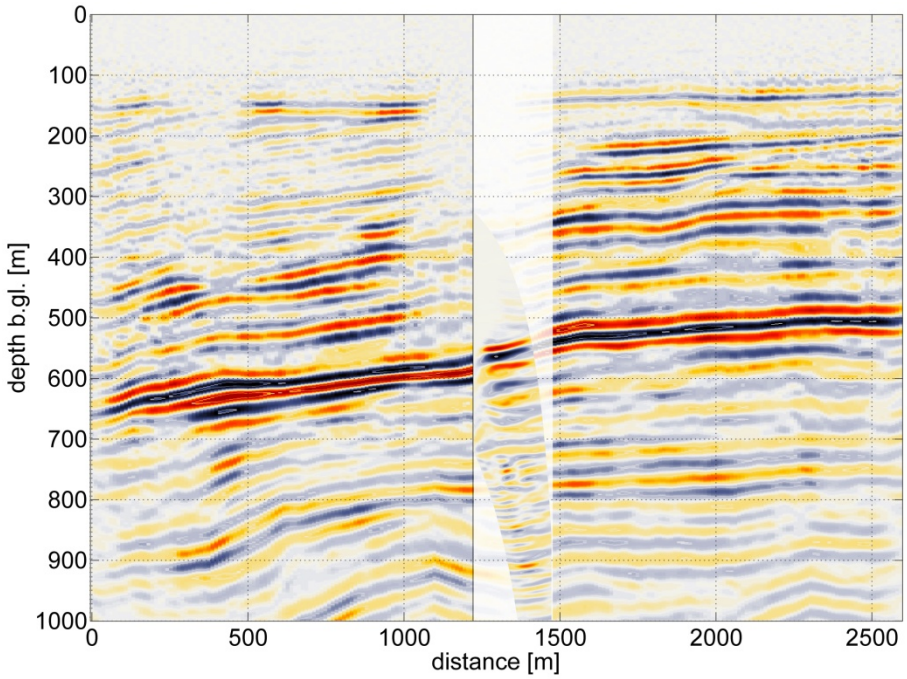

Figure 8.12 Offset VSP baseline, southern source point on line V1 (see Fig. 8.11) inserted for comparison into the 3D dataset at Ketzin (modified after Götz, 2012).

Passive seismics (including broadband recording)

In May 2008, the first measurements for passive seismic monitoring commenced before CO_2 injection started. This was to assess the noise level in the two observation wells and to test the borehole instrumentation. Repeats were carried out in autumn 2009 and also in February 2011 under pressurized conditions, with the help of a lubricator system and more robust instrumentation (Figure 8.13). In 2009, over a period of about 20 days, a 3-component highly sensitive downhole receiver was deployed for approximately 12 hours every night, while no active seismic or other field activities took place, with exception of the still running injection. To get an optimum data recording the passive seismic survey was acquired across a reservoir pressure change - i.e. injection stop-and-go regime of the CO_2 facility (Fig. 8.14 and Figure 8.15).

Figure 8.13 Left: The borehole instrument of Vibrometric (Finland) deployed in the field experiment of autumn 2009. Right: The wireless self-standing recording system from ELGI (Hungary) with flash memory card for data storage, and a vertical geophone (Rossi, 2011).

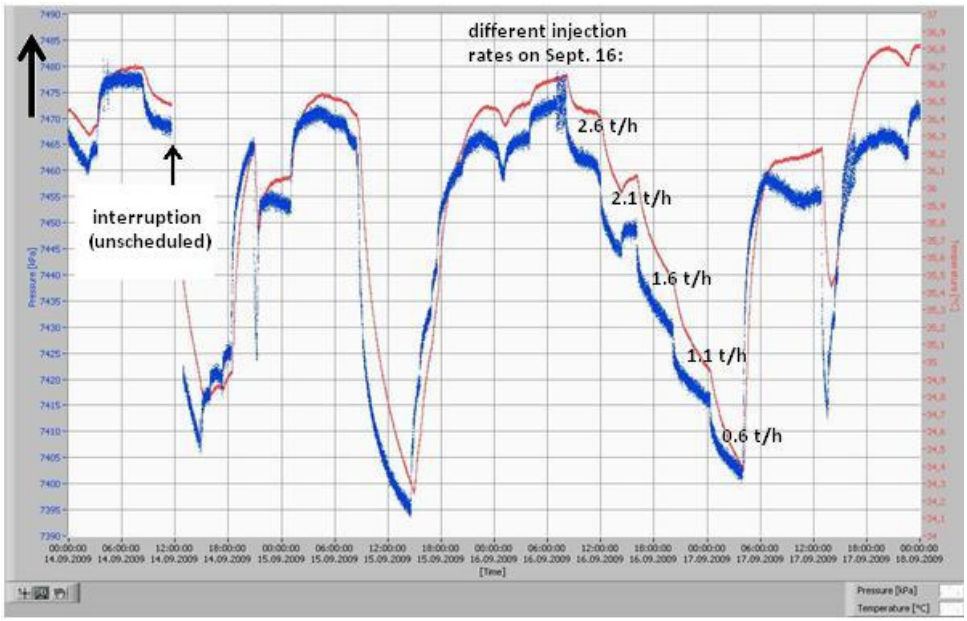

Figure 8.14 Design and implementation of a stop-and-go injection regime of the CO_2 facility: shut-in on 14-9-2009, and different injection rates on September 16th 2009, here plotted as pressure response (blue line, kPa) and temperature response (red line, °C) in the injection well at 550 m depth. A pressure difference of ~0.8 bar was passed during this test cycle.

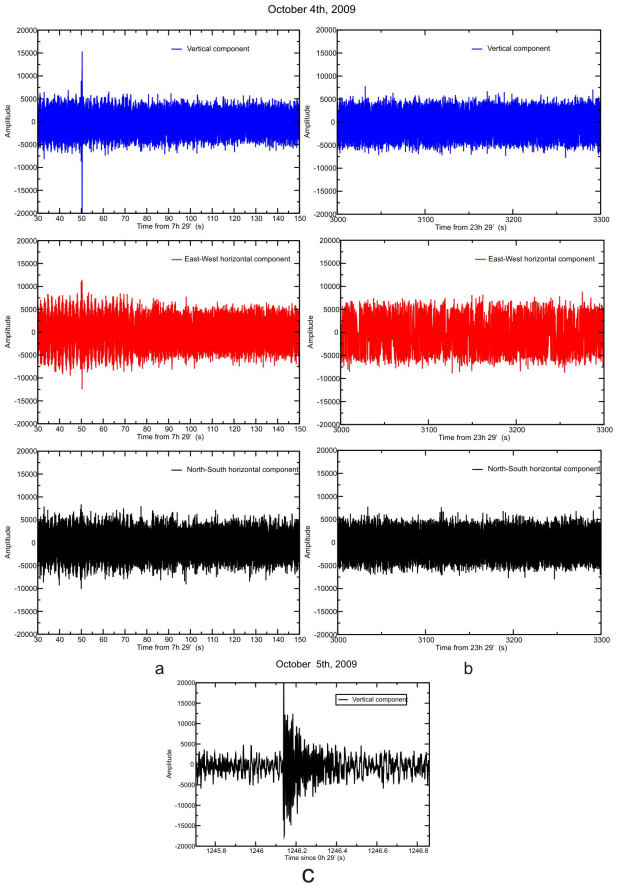

Figure 8.15 Examples of passive seismic recordings of the three component downhole instrument on October 4th, 2009 starting at 07:29 hrs (a,b), and on October 5th, 2009 starting at 00:29 hrs for the vertical component only (c). (Rossi, 2011).

In addition, an array of 50 cm deep buried seismic broadband stations (Güralp CMG3, frequency 0.1 - 50 Hz) was deployed at four selected places around the injection site which have been continuously recording from summer to autumn 2009 (Figure 8.16). The objective was to apply new interferometry methods using coda waves or even background noise as signal for regional tomographies, which means in our case the observation of the Ketzin site. A joint data evaluation considering all these measurements contributes to a better appreciation of the role of passive seismic monitoring in the assessment of the state and dynamics of a reservoir in CCS monitoring projects (Delatre *et al*., 2011).

Figure 8.16 Airborne photo of the Ketzin site with station locations (yellow pins, map source: GoogleEarth).The inset shows a buried broadband seismometer with isolation installation (left side), courtesy of M. Delatre, BRGM.

The frequency and passive interferometry analyses (Rossi, 2011) suggests that the signal content has changed between May 2008 (baseline) and September/October 2009 (repeat). However, due to operational constraints, i.e. deployment of a single downhole instrument and some modifications in the experimental setup, certain restrictions regarding the reliability of the results have to be considered. Therefore, it is not possible to unambiguously locate the possible source of noise, although it is determined slightly to the east of the injection well and approximately at the injection depth (Figure 8.17). To verify the results, and eventually prove the signal content changes, a repeat of the passive seismic experiment should be planned, using the same instrumentation as in October 2009.

Another insight drawn is that an efficient campaign, where several teams deploy the same logistics and wellbore equipment, could help to share the high costs. This is especially true for the lubricator technique required for monitoring in pressurised wells.

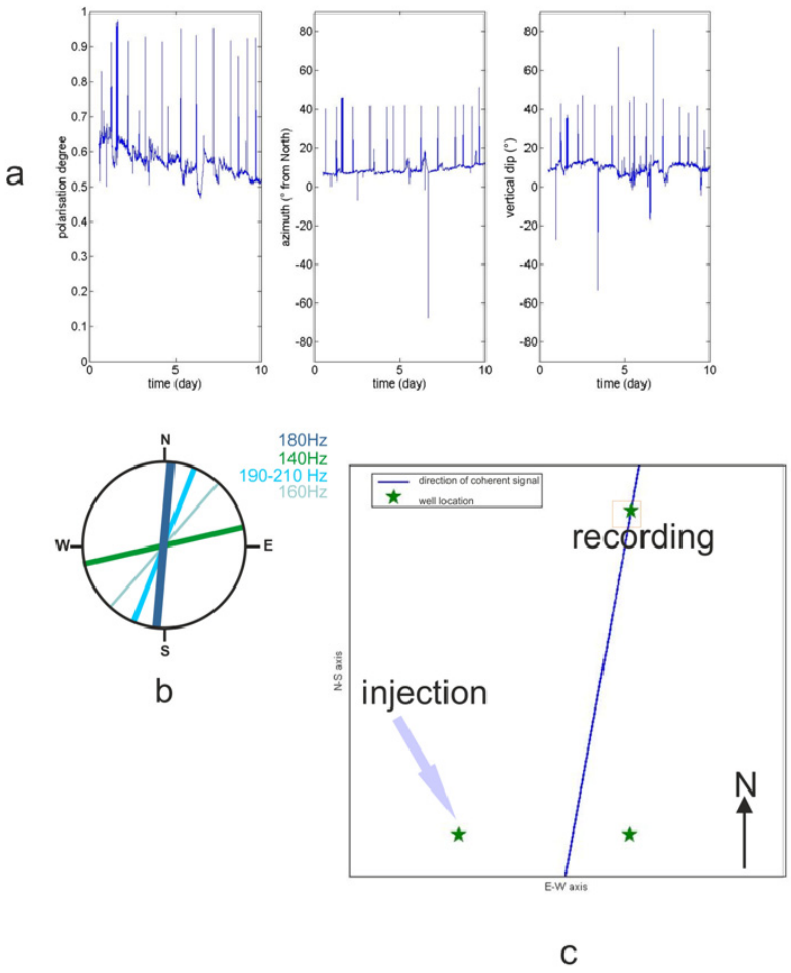

Figure 8.17 a) Polarization analysis along time: from right to left: polarization degree, azimuth, vertical dip. b) Stereogram of reporting the polarization directions for different frequency ranges, with segment thickness proportional to the modulus of the energy polarized in the various directions for the frequency range 140-210Hz; c) Sketch of the Ketzin site with the location of the three wells, and the line traced along the azimuth of the maximum eigenvalue of the covariance matrix.

Geoelectrical tools

For the Ketzin pilot site, a vertical electrical resistivity array (VERA) was developed together with other downhole sensors as "smart-casing" technology for the CO_2SINK wells. The array consists of 45 permanent electrodes (15 per each well), placed on the electrically insulated casings of the wells in the 590 m to 740 m depth interval with a spacing of 10 m. This layout has been designed according to numerical forward modelling assuming electrical properties of pre- and post-injection scenarios. The finally determined number of electrodes, their spacing along each well and the horizontal-to-vertical ratio of the image plane for each well and for the whole triangular setup results in a suitable compromise between resolution of CO_2 migration features and installation cost (Kiessling *et al.*, 2010; Schmidt-Hattenberger *et al.*, 2011).

In addition to the downhole measurement setup, temporary surface electrodes were also deployed for specific surface to surface, and surface to downhole measurements with in order to extend the area of investigation laterally about 1.5 km around the wells. The surface setup comprises 16 dipoles each 150 m long, arranged in 2 concentric circles of radii of 800 m and

1500 m. The aim of the combined measurements was to detect an indication of anisotropic effects in the CO_2 migration paths through the reservoir sandstone (Kiessling *et al*., 2010).

Time-lapse 3D images of the sub-surface resistivity distribution were generated from the electrical resistivity tomography (ERT) evaluation. The inversion results provide insight into the spatio-temporal plume migration and the corresponding CO_2 saturation in the target storage horizon. The present ERT results approximately match with results from other monitoring techniques employed at the site, as e.g. CO_2 signature detection by differences of reflection amplitudes from 3D seismic repeat (Fig. 8.18).Work is on-going to develop the ERT technique towards a system solution applicable for industrial-scale projects. Therefore, time-efficient data acquisition geometries, streamlining data processing and inversion are necessary preconditions (Bergmann *et al*., 2012).

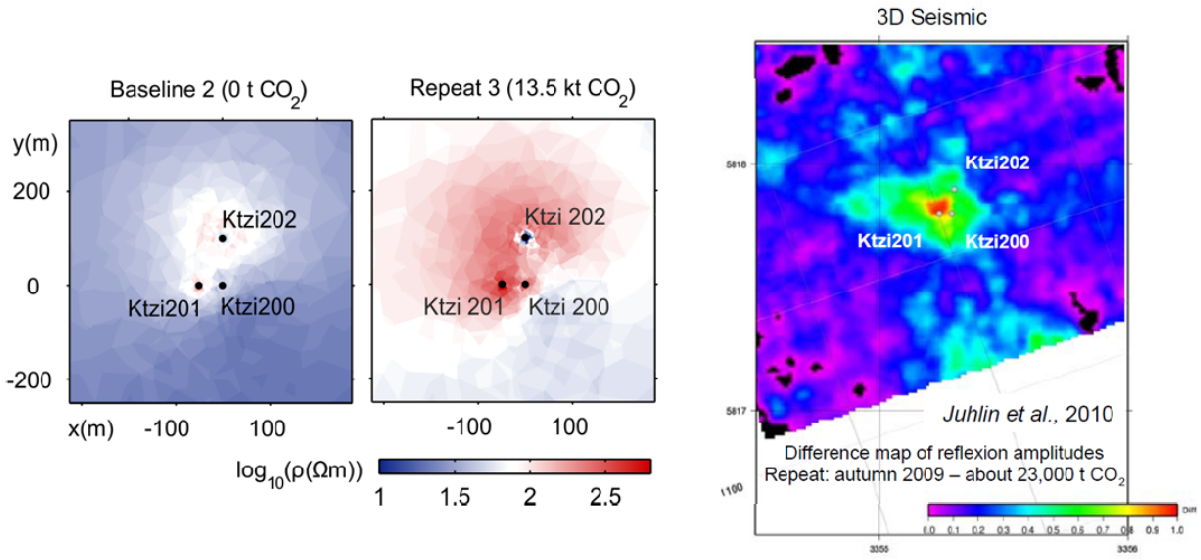

Figure 8.18 Comparison of plume imaging via surface-downhole electrical resistivity tomography (Bergmann et al., 2012) and surface 3D seismics at Ketzin (Juhlin et al., 2010).

Another geoelectrical approach on a larger spatial scale (range of some km) was provided by Controlled Source Electromagnetic (CSEM) surveys (Figure 8.19). In the frame of the CO_2ReMoVe project, the basic concept has been designated as long electrode mise-à-la-masse (LEMAM). Practically, this approach does not need special completion or equipment at depth as needed for electrical crosshole tomography. The method is designed to illuminate the deep CO_2 plume by a grounded injection of electrical current through the available boreholes (at Ketzin, the downhole electrodes were deployed), and to measure the resulting electric field at the surface. When the volume of the plume increases, the resulting electric field at the surface is modified. The surface field is recorded using several pairs of perpendicular electrical dipoles (~ 100m length) distributed in the area surrounding the boreholes, approximately 1 km centred on the injection well location.
A baseline measurement was carried out in the summer of 2008, followed by repeats in 2009 and 2010. The corresponding data evaluation was performed in time-lapse mode (Girard *et al*., 2011).
This work addressed the question whether or not geoelectric/electromagnetic (EM) measurements can reliably track the CO_2 plume propagation at different spatial scales. The CSEM campaigns offer the possibility to enlarge the area of investigation, and could also

provide a link to the 2D seismic star lines results (Ivandic *et al*., 2012). In general, from another land-based CSEM survey it was confirmed that a penetration depth of approximately 1 km can be reached, down to the flanks of the anticline and underneath the CO_2 bearing sandstone layer (Streich *et al*., 2011).

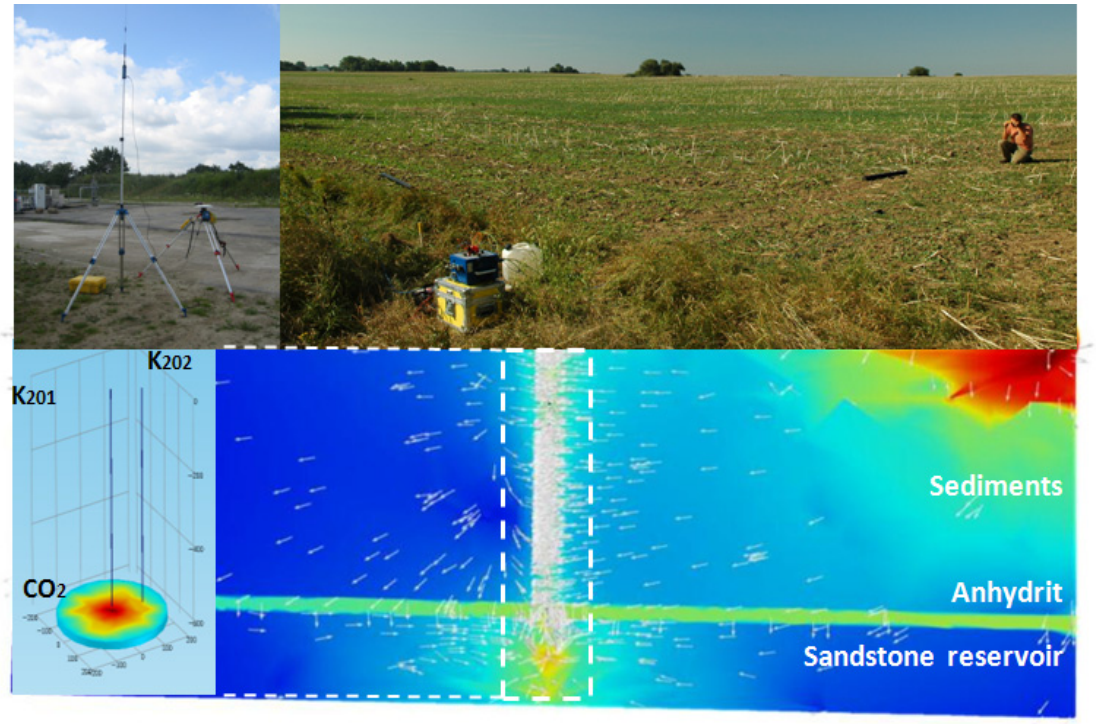

Figure 8.19 Schematic illustration of land-based CSEM. Receiver stations spread around the injection site are relocated by D-GPS (top-left) to measure the electric and magnetic field generated at the Ketzin ground surface (top-right)by a hole-to-surface current injection (bottom) disturbed by the CO_2 injection. Synthetic and also field data point out that the electric field spatial distribution is strongly controlled by a site specific feature: a thin, high resistive layer (~200 Ωm) of anhydrite causes the electric field to diverge from the boreholes (Courtesy of J.-F. Girard, BRGM).

It should be noted that the CSEM acquisition geometry at the Ketzin site does not exactly represent the original LEMAM method but an adequate adaptation, known as double mise-à-la-masse (MAM) in the literature (Girard *et al*., 2011). In the field surveys, the long electrodes were substituted by 8 borehole electrodes with distances of 10 m, which results in about 70 m vertical extent of current injection at the reservoir depth, crossing the CO_2 injection point.

The three Ketzin CSEM field campaigns have shown that it is possible to obtain good data quality, despite the high level of industrial electric noise caused by the neighboured power station, biomass plant, wind turbines, and gas pipeline with electrically pulsed maintenance. The processing of the time-lapse data has been represented more complex at this site, and there is the need to develop a specific approach for data inversion (Girard *et al*., 2011). The results clearly demonstrated the modifications of the electric field amplitude, and therefore the corresponding resistivity, induced by the CO_2 plume injection. While the 2009 survey highlighted the expected resistivity change at depth, the 2010 survey revealed a considerable and unexpected modification of the fluid content of the reservoir towards approximate initial

EM conditions (2008 baseline) (Figure 8.20 and Figure 8.21). It is considered that this change could be attributed to the lower CO_2 injection rate (2009-2010), which certainly induced a decrease of gaseous CO_2 (and its dissolution in the aqueous phase) in the vicinity of the borehole; and/or to a migration of the CO_2 plume in different parts of the reservoir.

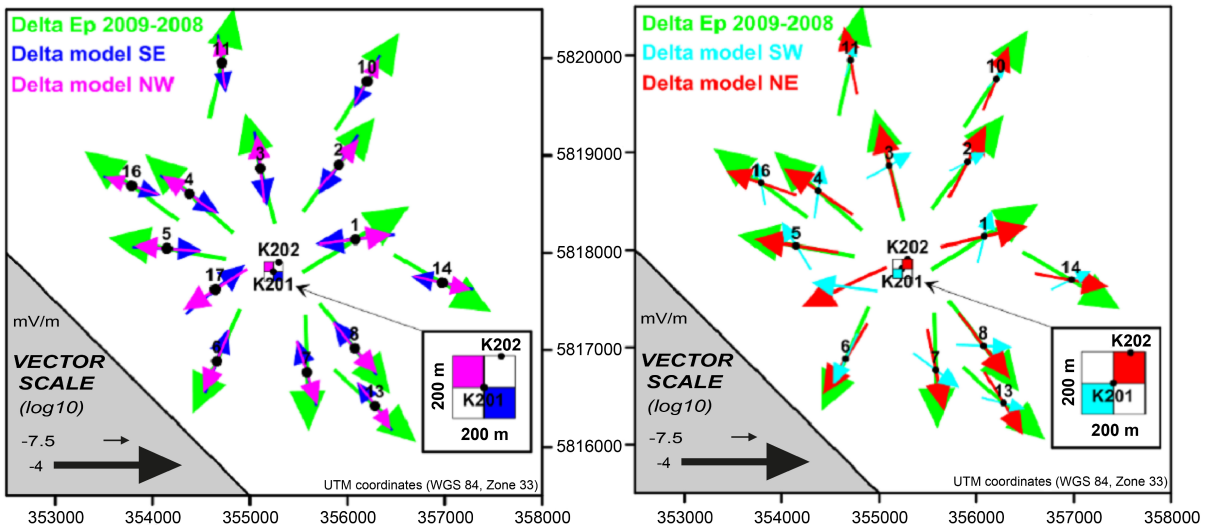

Figure 8.20 Resistivity residuals normalised to 1 Ampere current electric field (in-phase response Ep). Green arrows show Ep field data residual between 2009 and 2008 surveys. Purple, red and blue arrows show residuals between models with CO_2 plume (3 Ωm) respectively located NW and SE (left), and SW and NE (right) of borehole Ktzi201, and a model without CO_2 (1 Ωm). Insets zoom the modelled plume size and location. Best fit is obtained for the NE migration.

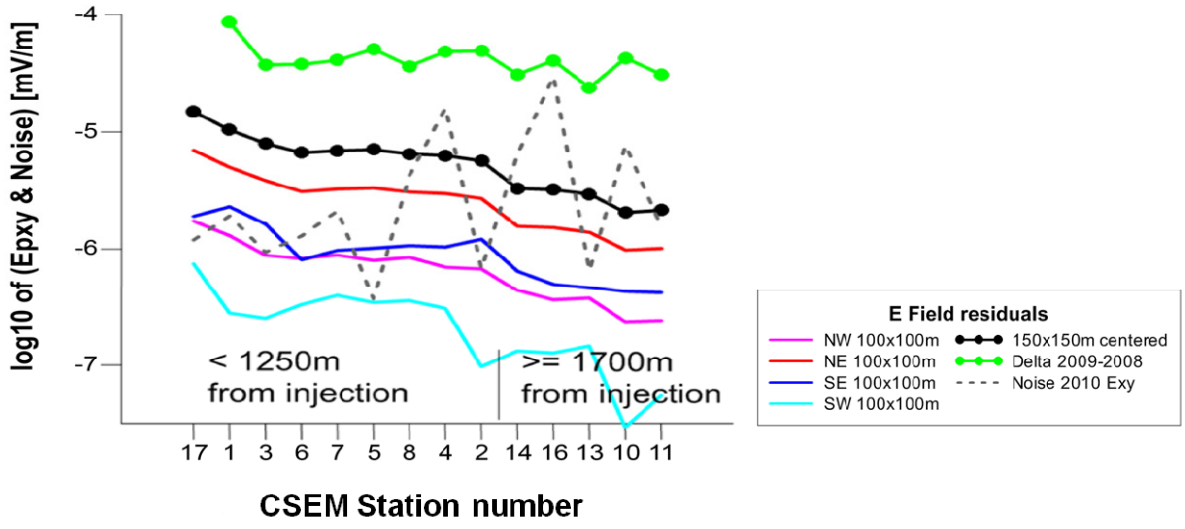

Figure 8.21 Resistivity residuals normalised to 1 Ampere current electric field (in-phase response Ep) vs. position of the receiver station. The green curve plots the Ep difference between the surveys 2009 and 2008. The purple, red and blue curves correspond to the Ep differences with the individual CO_2 plume models of Figure 8.18 (see insets there). The Exy 2010 noise (dotted line) shows that at greater distances from the boreholes the resolution of the residuals decreases but still remains significant.

Temperature monitoring

CO_2ReMoVe provided a distributed temperature sensing (DTS) monitoring system for the Ktzi 201 3.5″ injection tubing, in addition to the already existing behind-casing DTS at the 5″ steel casing of the three Ketzin wells (Figure 8.22). This additional tool has enabled high quality continuous temperature measurements to better understand the physical properties of the injected CO_2 stream and their temporal changes during shut-in and re-start processes (Schmidt-Hattenberger *et al*., 2009).

The fibre optic sensor cables of the DTS systems provide temperature profiles to be measured continuously along the entire length of the wellbores with high temporal and spatial resolution, either for the injection behaviour (3.5″ string) or for the formation behaviour (5″ casing). To enhance the thermal signal and improve the monitoring of brine and CO_2 transport, active thermal perturbation experiments were performed using an electrical heater cable installed adjacent to the DTS cables (Freifeld *et al*., 2009). Apart from long-term temperature monitoring during the injection process, the DTS data from the 5″ casing also allowed for better analysis of the process of casing cementation (Henninges *et al*., 2009). The monitoring of cementing operation is crucial to ensure the required sealing capability of the borehole completion for CO_2 storage wells.

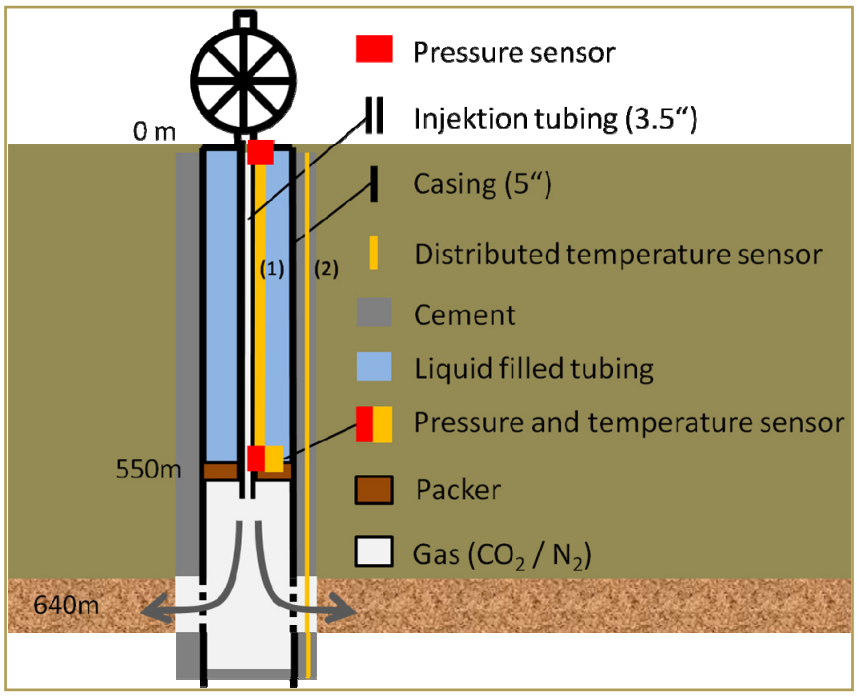

Figure 8.22 Sensor instrumentation of the injection well Ktzi201. Two DTS systems are operating in this well: (1) along the 3.5″ injection tubing for temperature monitoring of the CO_2 stream behaviour, and (2) along the 5″ steel casing for temperature monitoring of the formation behaviour. Figure re-drawn and modified after Wiese et al., (2011).

Since the start of CO_2 injection, the temperature distribution along the injection well and the two observation wells is recorded continuously. In Figure 8.23, temperature data extracted for particular depths of the three Ketzin wells for the initial two-month period after start of injection are shown (Giese *et al*., 2009). Temperature changes in the injection zone are in the order of 5 to 10 °C. In the two observation wells temperature changes of up to about 1.5 °C were measured within the reservoir section. A temperature increase of about 0.5 °C was observed at the reservoir level (upper filter screen) in Ktzi 200 prior to the time of breakthrough of CO_2 detected with the gas membrane sensor (GMS). The temperature anomalies detected with the DTS sensor cables allow analysis flow processes within the wells and phenomena related to the spreading of CO_2.

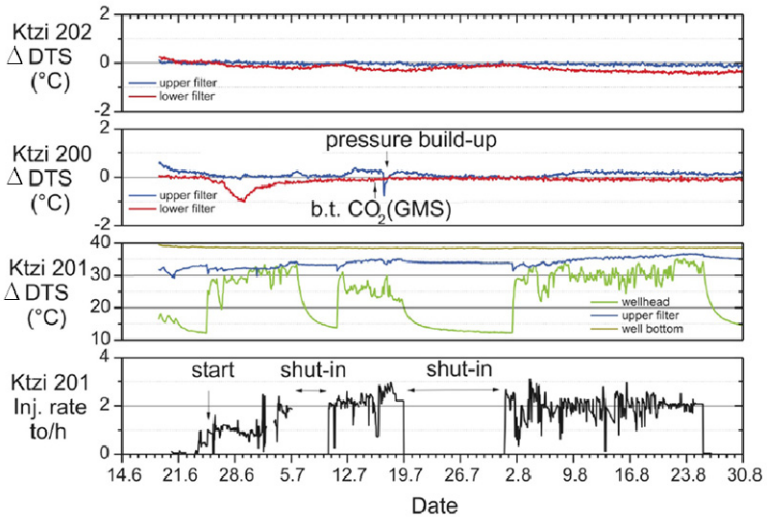

Figure 8.23 DTS monitoring along the 5″ casing during injection, with wellhead temperature of about 36 °C. Injection rates and differential DTS temperatures in injection well (Ktzi 201) and temperature changes at the filter screens in the two observation wells (Ktzi 200 and Ktzi 202). The breakthrough time (b.t.) of CO_2 detected with GMS sensor in Ktzi 200 is marked with an arrow. The original formation temperature was 33°C (modified after Giese et al., 2009).

Regarding the injection tubing, the DTS data evaluation was focused on typical stages of operation: shut-in phase / steady-state phase / restart phase of CO_2 injection (Figure 8.24). Detailed comparison between these operational stages provides insight into the stability of the injection process, its time response, and the energy consumption of the injection control. Furthermore, the DTS monitoring yields indirect information about the state of the injection tubing surface, which can be affected by corrosion via the CO_2-brine subsurface conditions. Therefore, the lifetime of the tubing and the possibly occurrence of leakage points can be monitored. This contributes to the well integrity and risk mitigation for the long term operation of the injection process until the abandonment phase.
In addition to the operational information provided, the DTS data has been used to recalculate a continuous pressure profile along the entire length of the injection well. The data allow the calculation of the thermodynamic properties of the CO_2 inside the injection well as well as potential phase transitions during the injection process. Due to compression, a heat flux establishes between the injection well and subsurface which can be quantified based on the thermodynamic state.

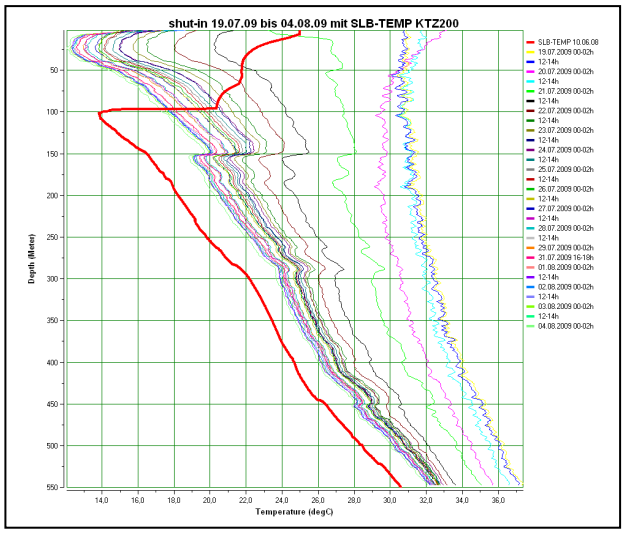

Figure 8.24 DTS measurements for the shut-in period 19/07/09 – 04/08/09. Note how high injection temperatures relax towards the geotherm over the observation period (red line approximates to the geotherm below ~ 100 m depth).

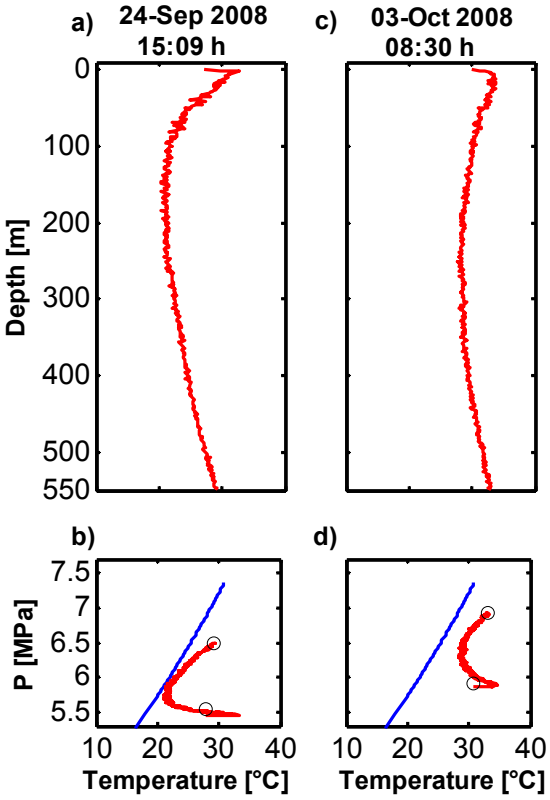

Figure 8.25 Profiles from the injection well Ktzi 201. a) and c) are measured temperature profiles; b) and d) show the thermodynamic state with temperature and pressure. The grey line is the CO_2 phase boundary, the black line the calculated phase state and the circles are measured state variables at 0 and 550 m. a) and c) also refer to the temperature axes from b) and d).

Figure 8.25 illustrates two snapshots from the injection well Ktzi 201 directly after injection restart (Figure 8.25a, b) and nine days later (Figure 8.25c, d). The Figure 8.25a and c present the temperature profile measured with the DTS system. The temperature at the upper 3 to 5 m is biased because it is affected by the atmosphere and, therefore, smaller compared to deeper regions. From a depth of about 5 m the temperature decreases to a minimum value located between 150 and 300 m. This occurs because the CO_2 is heated, and the heat is transferred to the subsurface. As the geothermal temperature increases, the heat transfer is reduced and the temperature rises due to compression and the Joule-Thomson effect. The temperature increases with the duration of injection (compare Figure 8.25a and c).

The thermodynamic state is clearly subcritical (P_{crit}=7.38 MPa, T_{crit} = 31.1°C) in the gaseous region for the measurement points at 0 and 550 m (Figure 8.25b). Between these points, however, the temperature is lower, the pressure is different and the thermodynamic state is close to condensation. As injection continues, the borehole is heated and also the pressure increases. For regular operation, as shown in Figure 8.25d, the injection well between 0 and 550 m is clearly in the gaseous region with a safety margin of 3 °C to the condensation line.
These thermodynamic investigations provided insight into the phase behaviour of CO_2 in the injection well. They represent a substitute method instead of the camera inspections which have been carried out in the Ktzi 200 and in the Ktzi202 wells. For the Ktzi 201 well, the video camera cannot pass the special well completion, i.e. the 3.5″ narrow injection tubing and its safety valve installation; both represent technical constraints.

Pressure monitoring

A Fiber-Bragg-Grating (FBG) based pressure sensor has been installed in the well Ktzi 201 at the end of the injection tubing string (Figure 8.22). Based on the excellent references from more than a decade of applications in the oil and gas market the decision was made in favour of this fiber optic technology (Overton, 2011). The sensor operates as single-point pressure gauge and provides real-time values of wellbore pressure and wellbore reference temperature at the end of the injection string at 550 m depth. The pressure data from the so-called pT-gauge are extrapolated with the commercially available ASPEN PLUS program by AspenTech applying a Peng-Robinson equation of state (EOS) to the depth of 630 m (top of the injection zone). This adjustment of the pressure measurements allows direct comparison with the reservoir simulation results. The gauge is temperature compensated, and is designed to have a long life time at high environmental temperatures. The maximum continuous operating conditions of the transducer are 150°C and 13.7 MPa.

The main application of the sensor is the real-time monitoring of reservoir pressure during the injection process, and control of the well in order to avoid critical situations during CO_2 injection operation. An additional key application of the monitored data is in history-matching (Figure 8.26) to determine reservoir injectivity and capacity.

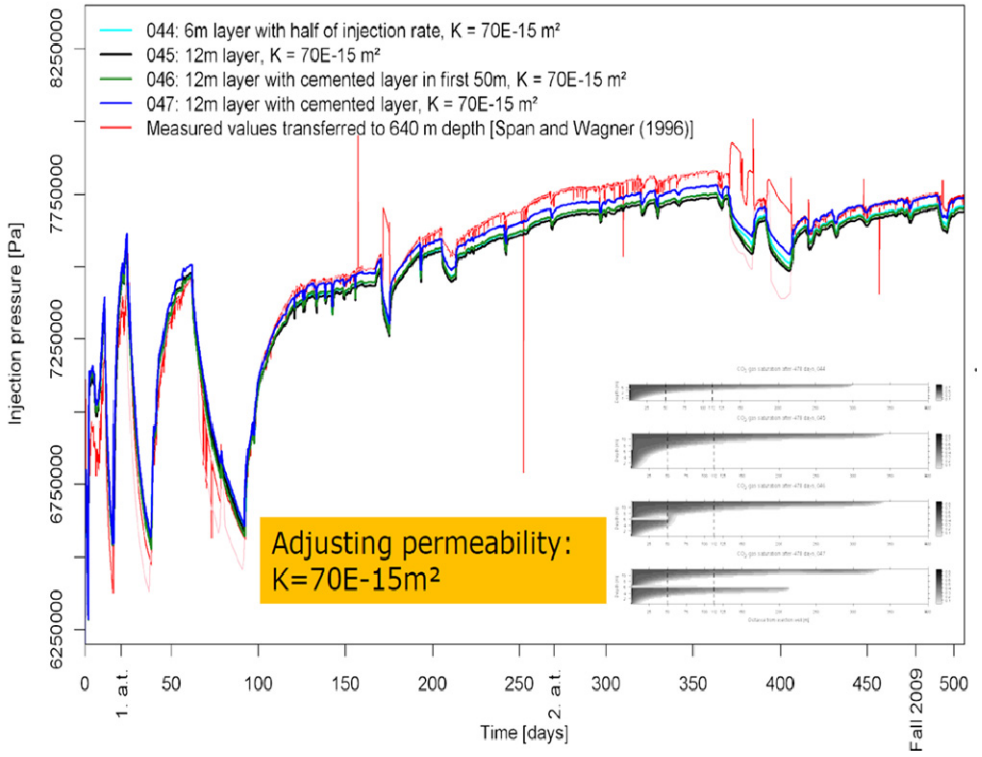

Figure 8.26 Pressure history-matching at Ketzin by adjusting reservoir properties (Lengler, 2010).

Geochemical monitoring

For the real time *in situ* determination of CO_2 and other gases an innovative geochemical monitoring tool, the so-called gas membrane sensor (GMS), was developed and applied in the two observation wells. The technique is based on a phase separating silicone membrane, permeable for gases, in order to separate gases dissolved in borehole fluids, water and brines. Argon is used as a carrier gas to conduct the collected gases through capillaries to the surface. Here, the gas phase is analysed in real-time with a portable mass spectrometer for all permanent gases. In addition, gas samples may be collected for more detailed investigations in the laboratory (Zimmer *et al*., 2011a).

Downhole sampling and online determination of gases dissolved in brines using the gas membrane tool was successfully applied from the start of injection (June 2008) to the arrival of CO_2 at Ktzi 202 (March 2009). With the GMS technique even minor concentrations of stripped gases like helium, hydrogen, methane and nitrogen during CO_2 injection were determined (Zimmer *et al*., 2011a).

The arrival of CO_2 into the first observation well, Ktzi 200, 50 m from the injection well, was recorded after the injection of about 531 tonnes, and the arrival of CO_2 into the second observation well, Ktzi 202, at 112 m distance, was recorded after the injection of about 11000 tonnes (Figure 8.27). It is notable that the injected Krypton tracer was detected about one day before the CO_2 was measured.

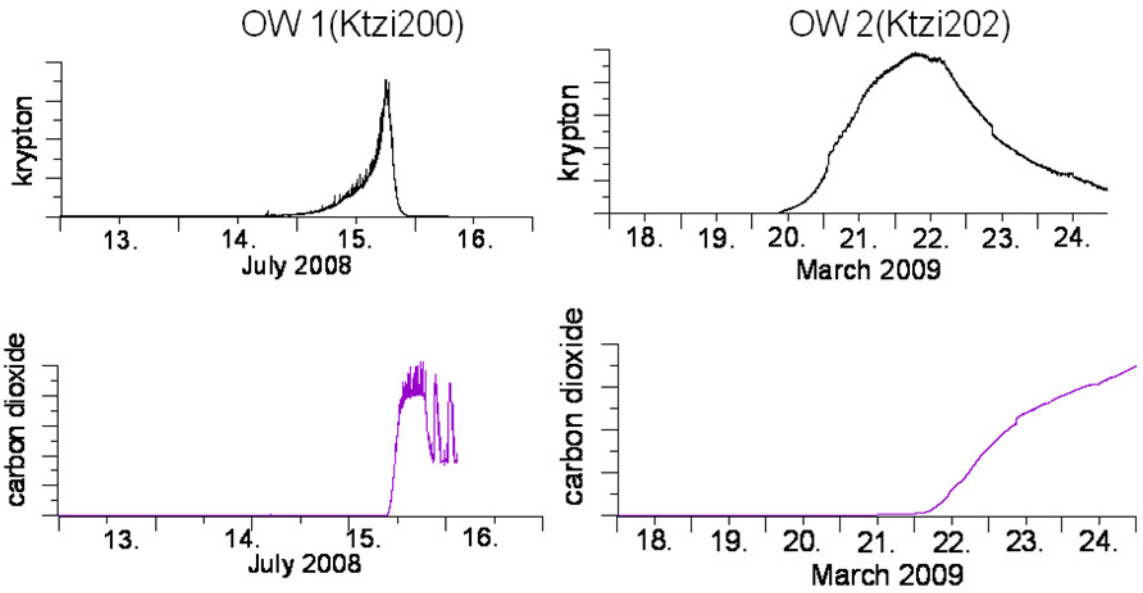

Figure 8.27 Breakthrough of Krypton tracer and CO_2 at the two monitoring wells (Zimmer et al., 2011a).

In addition, a comprehensive program for long-term geochemical monitoring at the surface was set up for safety and environmental monitoring purposes. CO_2 soil gas flux, soil moisture, and temperature measurements were conducted once a month during a 6-yr period. Furthermore, soil samples were analysed for their organic carbon and total nitrogen contents (Zimmer *et al*., 2011a).

Microbiological monitoring

The main objectives of the microbial monitoring at Ketzin were to:

- locate, identify and analyse the composition and activity of the subsurface microbial community,
- unravel the origin and fate of dissolved organic matter (potential substrates and metabolites of microorganisms), and
- characterise microbial life in extreme habitats and its influence on the precipitation and dissolution of minerals as well as their impact on the technical effectiveness of the CO_2 storage technique (Morozova et al., 2010; Zettlitzer et al., 2010; Wandrey et al., 2011).

In order to investigate the processes in the deep biosphere, rock cores and fluid samples were collected from the reservoir. Beside halophilic bacteria the sulphate reducing bacterium (*Desulfotomaculum salinum*) was found, which is known to be involved in corrosion processes (Morozova *et al*., 2011). Reactions between the microorganisms and the minerals of both the reservoir and caprock may cause changes in the structure and chemical composition of the rock formations, corrosion at the casing and the casing cement around the well.

8.3 Monitoring data acquisition

The Ketzin monitoring tools and their corresponding datasets can be categorised as deployed in permanent and non-permanent configurations (Tables 8.1 and 8.2).

8.3.1 List of data types and resolution

Table 8.1 Ketzin monitoring: non-permanent techniques

Selected tools (Method)	***Application***	***Aim***	***Area covered*** ***(total area that can be surveyed)***	***Resolution*** ***(volume of support for the measured value)***
Seismic	cross-hole	- detection of CO_2 - geometry of CO_2 plume - extension of CO_2 plume	between observation wells	~ 1 to 2 m
	surface to downhole (VSP; MSP)		300 m around injector	~ 10 to 20 m
Juhlin *et al.*, 2007 **Juhlin *et al.*, 2010** **Yang *et al.*, 2010** **Bergmann *et al.*, 2011** **Lüth et al., 2011** **Rossi , 2011**	surface to surface (2-D star; 3-D)		12 km^2 around injector	≥ 10 m (vertical)
	passive downhole		100 m around injector	n.a.
Electrical Resistivity Tomography **Controlled Source Electromagnetic (CSEM) Measurements** **Girard *et. al*, 2011** **Bergmann *et al.*, 2012**	surface to down hole (resistivity)	- indication of anisotropy in migration of CO_2	~ 1.5 km around injector	max. 5 m in the near-wellbore area
Logging **P-T, Reservoir Saturation Tool (RST)** **Norden *et al.*, 2010** **Henninges *et al.*, 2011a,b**	in-well	- in-well conditions (P, T, fluid flow) - near-well CO_2 saturation	near-well cm to dm	~ 0.15 to 0.6 m
Heat-pulse experiments **Freifeld et al., 2009**	in-well	- detection of fluid flow and CO_2	near-well cm to dm	1 m
Down hole fluid sampling **Morozova *et al.*, 2010** **Wandrey *et al.*, 2010**	in-well	- organic and inorganic chemistry - CO_2-fluid-rock-biocenosis interactions	in- and near-well	point measurement (=sample volume)

Table 8.2 Ketzin monitoring: permanent techniques

Selected tools (Method)	***Application***	***Aim***	***Area covered***	***Resolution/ detectability***
surface monitoring **Zimmer *et al.*, 2011b**	measurement station network	- surface CO_2 flux	4.5 km^2 around injector Depending from mesh-size (number of stations)	Res.: 1µmol/m^2 s Detectability dependent on the seasonal natural CO_2 flux
Multi-parameter monitoring in groundwater wells **Norden, 2011**	shallow wells	- mass transport meas. via pH, p, T, CO_2 concentration and water level		under investigation
P-T monitoring **Würdemann *et al.*, 2010**	in-well	- pressure and temperature within injection well at depth	in injection well	point measurement at the end of injection string
DTS **Henninges *et al.*, 2009**	in-well	- temperature distribution within wells	in-well and nearest-well area; cm to dm	1 m
gas membrane sensor **Zimmer *et al.*, 2011a**	in-well	- gas composition in well/at depth	mg/l, restricted to sampling point Area, where free gas bubbles occur.	GMS can only detect free gas bubbles occurring in the wellbore. Solved CO_2 cannot be detected.
ERT **Kießling *et al.*, 2010b** **Bergmann *et al.*, 2010** **Schmidt-Hattenberger *et al.*, 2011**	cross-hole	- detection of CO_2 - extension of CO_2 plume	~ 30 m around wells	~ 5 to 10 m
Passive seismic monitoring by buried receivers (TNO array) **Arts *et al.*, 2011**	permanent buried sensor array	- migration of CO_2	injection site	~ 5 m (vertical)

8.3.2 Timing and quality

In Figure 8.28, a schematic of the time history for a selection of relevant field campaigns is presented, which covers the so-called non-permanent monitoring tools. The development of the in house-software CO_2DataTool (toolbox for treatment and processing of data from CO_2-injection operation) proved to be very beneficial for timing and analysis of the acquired field data sets wich could be integrated with their corresponding operational data as e.g. CO_2 pressure, CO_2 temperature, and CO_2-flow rate.

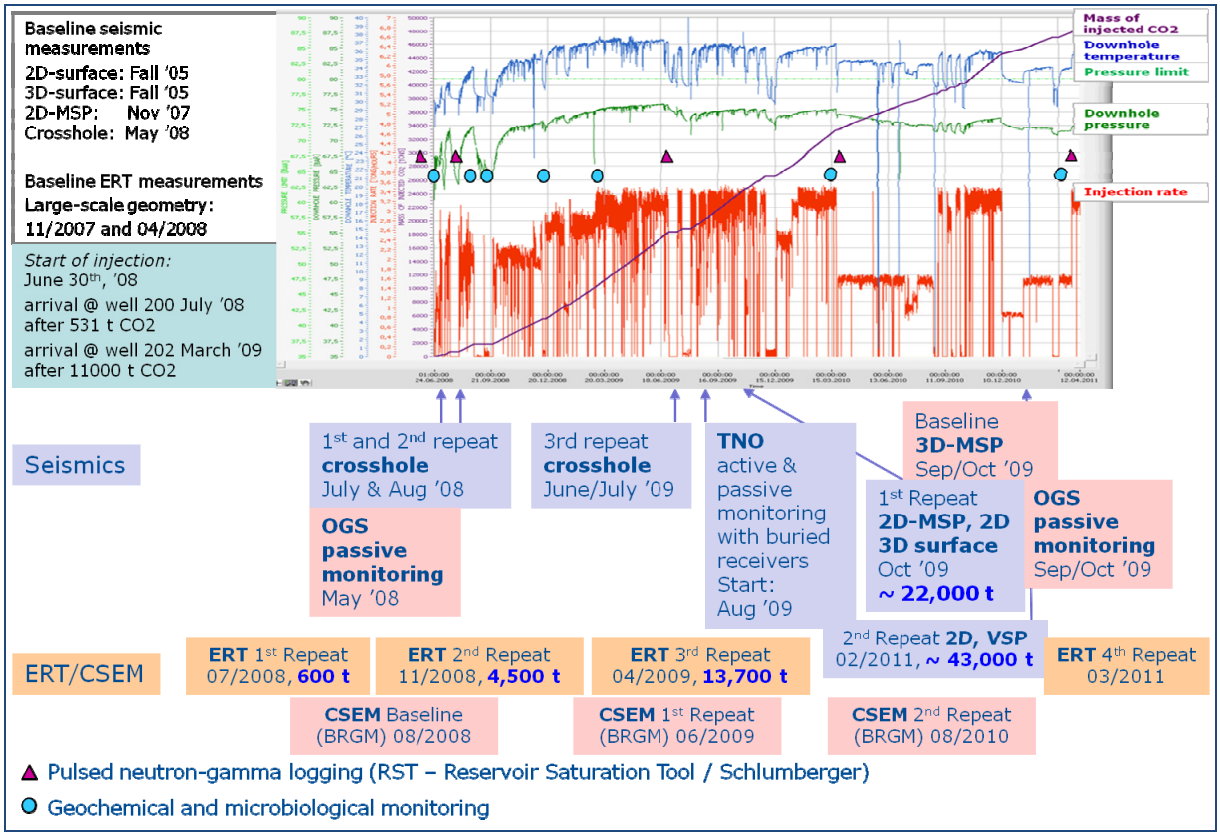

Figure 8.28 Timing of the non-permanent monitoring tools (selection) from June 2008 until April 2011.The CO_2ReMoVe supported campaigns are marked in pink colour. The CO_2 injection history and its relevant operational parameters has been visualized by the Inhouse-software CO_2DataTool (LabView based).

A brief overview on the performance of the various tools is given in Table 8.3., which stands in a figurative sense for the quality of measurements.

Table 8.3 Overview of tool performance

Tool / Method	***Physical quantity considered / Criterion***	***Objective achieved?***	***Remarks / Operational difficulties***
RST Log	CO_2 saturation	Saturation conditions in the near-wellbore area determined	Complex numerical procedure has to carried out for the logged data due to specific conditions (CO_2, cementation circumstances) Limited significance by very short penetration range.

Bottomhole pressure and temperature	Observation of reservoir pressure within the range of the defined pressure limit (82 bar)	Precise and reliable on-line detection of P-T- data.	Industrial measurement system, with good long-term stability.
Seismic measurements	Seismic velocity/ P-wave velocity decrease.	Plume dimension determined approximately. Volumetric quantification still under investigation	Sources and receivers of the high-resolution crosshole measurements are placed in the Ktzi200-Ktzi202 plane for technical reasons. Not optimal.
ERT	Resistivity / resistivity increase.	Plume migration detected by time-lapse measurements, volumetric evaluations (transfer from resistivity mapping to saturation profiles) still under investigation	Vertical electrode array fit is not optimal to the reservoir geometry (very thin sandstone layers ~ 25 m), was selected due to technical and economical constraints.
Active DTS	Temperature /deviation from linear trends, anomalies	Precise measurements of downhole conditions.	Very short penetration range.

8.4 Performance assessment (PA)

In the frame of the EU FP6 CO_2SINK project, a comprehensive set of expert analyses and studies has been performed to establish migration scenarios and a worst case scenario, and to establish a Safety Case for Long Term Storage Containment at the Ketzin site (Flach et al., 2008).
For an early assessment of the capacity and injectivity prior to drilling of injection and observation wells, a reservoir model was constructed based on the existing data. This model was used to illustrate the migration pattern and distribution of CO_2 during and after the predicted injection period.
A worst case scenario, assuming a fault pathway between the CO_2 storage reservoir and the retired natural gas storage reservoir above, was analysed for a maximum injection volume of 60,000 tons CO_2, using the pre-drill reservoir model.
When the acquisition and interpretation of the new 3D seismic data supplied new structural maps, and the three wells were drilled giving important petrophysical data, the reservoir model was updated with this information. This model was then used to predict CO_2 migration and arrival time at the observation wells. Site performance data have been collected since that time and this represents the primary source for further performance assessment updates.

8.4.1 Reservoir modelling and flow simulation studies

Dynamic flow modelling of the CO_2 injection at the Ketzin site was performed at different stages depending on increasing data availability with time. The initial work in 2006 was based on sparse data prior to the new 3D seismic acquisition and prior to drilling of new wells, and was carried out to investigate the capability of the structure to store the scheduled amount of CO_2, and for looking into the larger scale migration of the injected CO_2 including a period of 20 years equilibration after injection ceased. Later updates of the reservoir model as more data became available were used for further predictions and for comparison with the monitoring data obtained during the operation of the site.

Table 8.4. List of reservoir model versions.

Reservoir model versions	***Well data***	***Structural data***	***Supplementary data***
V_0.1 **For feasibility and migration predictions**	1 old well 3.4 km from injection site (Ktzi_163/69)	Existing old 2D lines in region interpreted	Initial conceptual depositional model. Model version finalised and published 2006.
V_3.0 **For arrival time simulation and comparison studies**	3 new wells drilled (Ktzi_200, 201, 202)	New 3D seismic survey interpreted	Refined depositional model and well data on facies and porosity introduced in model. Model version finalised 2008.
V_4.0 **For long term migration and equilibration studies**	Same data and geo-model as V_3.0, but gridding in reservoir model adjusted for simulation of longer distance migration analysis		Model version finalised 2009.

Modelling of CO_2 storage sites in deep saline aquifers is usually associated with very low data density. This places weight on prior regional understanding of the depositional setting to support the understanding of the reservoir architecture. This framework is then populated with conceptual models drawing on experience with analogues and inspiration from literature examples.

As for other reservoir developments the modelling is an iterative process as observation from the site characterization arrives, and as special monitoring data are retrieved as part of the storage site development. The Ketzin pilot site in Germany has been through these different stages of development and is still developing. One stage of this history has involved the creation of a probable geomodel to be used for prediction of reservoir behaviour.

The injection horizons are sandstones of the Upper Triassic (Keuper) Stuttgart Formation with variable thickness. The Stuttgart Formation is lithologically heterogeneous, consisting of sandy channel-facies rocks with good reservoir properties alternating with muddy flood plain facies rocks of poor reservoir quality. In distinct areas, the channel sandstones are more frequent, reflecting channel belt fairways. The lateral extension of the channel belts, formed by amalgamation of individual fluvial channels, is assumed to be highly variable. The upper

seal of the Stuttgart Formation is the Weser Formation, consisting mainly of clayey and sandy siltstones, which alternate with carbonates and evaporites.

Reservoirs in fluvial sequences are generally challenging to model for reservoir properties. This is due to the large contrasts between the different facies associations, the distinct architecture, and the different heterogeneity within each facies association. Therefore a combination of different geostatistical methods is necessary to reflect the multitude of variations. This combination is illustrated for the Ketzin site. For this site modelling has been chosen a 2-step process using first an object modelling tool generating stochastic models of sinuous channel belt bodies within a back-ground matrix. Then the heterogeneity within each channel belt is produced by using a Sequential Gaussian Simulation (SGS) scheme to populate with petrophysical properties of porosity and permeability. The SGS is used to generate variability with a geometry/size mimicking the patchy occurrence of pointbar and channel fill porous sands within the channel-belts.

For defining input to the object based modelling, the overall geological setting as an intra-continental fluvial plain, assumption of meandering geometry, and a generally North to South transport direction, have directed the input for the object modelling procedure. The width of the channel belts was set as a range from 100 to 1600 m, guided by the analysis of range of thickness for the pointbar deposits of between 1 and 8 m. The relation between channel belt width, w, and channel thickness, t, has been reported as the ratio w/t = 200 (Bridge and Leeder, 1979). The channel belt widths used in the present model are between 100 and 1600 m based on the channel sand thickness of 1, 4 and 8 m and on the relationship w/t ranging from 100 to 200. This input conforms to the average relation as given by Bridge & Mackey (1993).The sinuosity of the channel belt is described by an amplitude of 400-1000 m and a wave-length of 5000-9000 m. This is not very well supported by data or analogues from literature.This uncertainty about establishing input parameters for fluvial system models have been emphasized by Miall (2006), and therefore the models must be supplemented by local data if available, and a range of scenarios should ideally be developed to study the effects on the flow behaviour investigated. The circumstances for the Ketzin project have only allowed a very limited investigation in such a procedure.

The first simplified reservoir model version 0.1 (Figure 8.29) was based on a preliminary static geological model constructed from very sparse data (Förster et al., 2006), and turned out to be not suitable for predictions at local scale, but only as a general indication on the overall behaviour of the plume of injected CO_2 (Frykman, 2009b). The lack of prediction at local scale is a consequence of the few hard data points and therefore increasing uncertainty away from these points, in combination with the very high property contrasts for this specific environment of fluvial deposits.

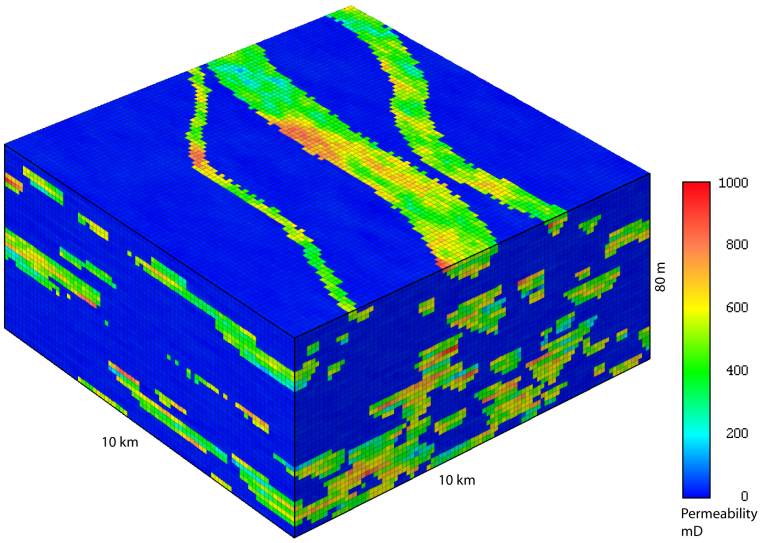

Figure 8.29 Permeability in the static model version 0.1 for the injection site area of 10x10 km, with variations reflected only inside the channel-belt facies. The channel sand has been assigned a permeability distribution with a mean of 500 mD and the floodplain has been assigned a constant permeability of 0.1 mD. (Förster et al., 2006).

The update incorporating the data from the three wells drilled facilitated a new facies model for the full reservoir model (Figure 8.30)

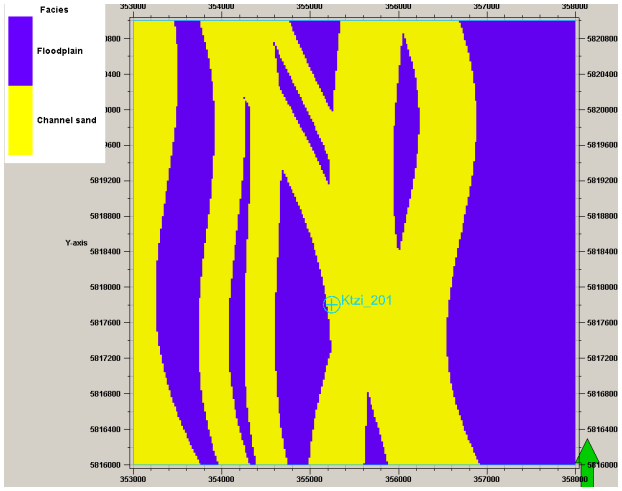

Figure 8.30 Facies model in the updated geo-model of 5x5 km areal size showing channel-belt geometry in layer 14 in the model.

The interpretation of the well log data from the three new wells drilled has been described separately (Norden et al., 2010). For each of the two facies types (channel/floodplain) the porosity data have been analysed for distribution (histogram), which then has been smoothed and used for a target distribution to use in the petrophysical modelling of porosity with SGS within each facies defined by the channel-belt objects and background separately.
Modelling of the porosity using the SGS algorithm is done with variograms of 400-800 m range to create patches that could mimic the pointbar deposits in the channel-belt interior, and layering thickness of an average of 2 meter. The size range of pointbar deposits have been inspired by mapping of other fluvial system deposits. The illustrated examples originate from the Widuri oil field, Java Sea, where 3D seismic data attributes (Figure 8.31) have been used to delineate high porosity sands (Carter, 2003). The seismic images show a range of features related to point-bar geometry and the patchy distribution of porous sands. The interpreted shapes and dimensions are consistent with observations of modern-day examples.

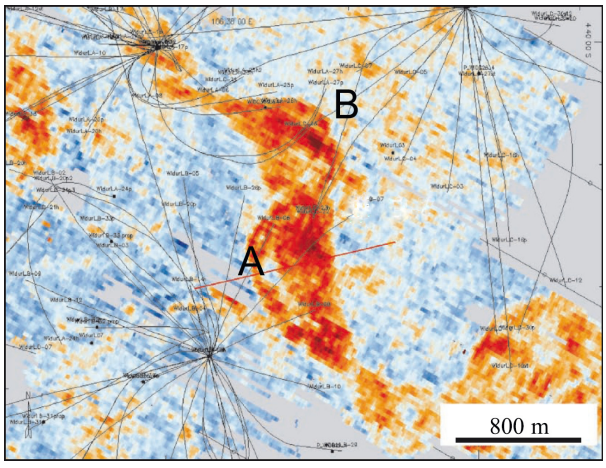

Figure 8.31 Amplitude image of unit in the Widuri field showing outline of porous sands. (Modified from Carter, 2003).

The updated version 3.0 static model of the Ketzin reservoir includes the new structural maps from the new 3D seismic survey interpretations (Juhlin et al., 2007), and well data from the three drilled wells (Norden et al., 2010). The overall conceptual model of depositional environment as a fluvial setting with channel-belts developed by meandering river deposits has not been changed, but refined by adding more information from analogue studies (Figure 8.32). The detailed well data interpretations were used for input on depositional facies, porosity and modelling of permeability (Norden et al., 2010).

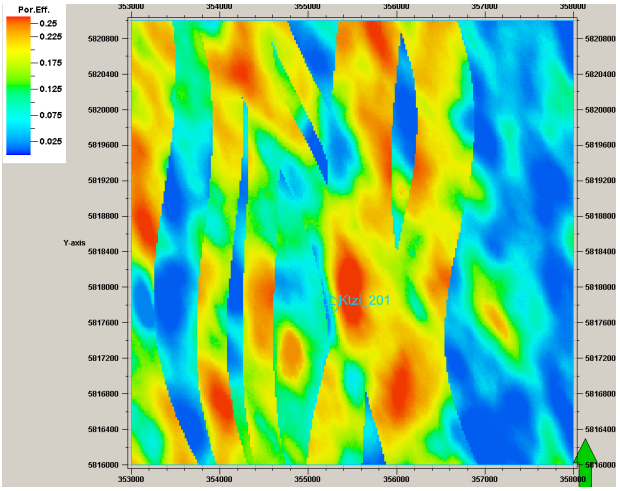

Figure 8.32 Effective porosity in layer 14 in the Ketzin model.

Based on this update with additional data from the wells, the SGS was used to model a new porosity model for total porosity and effective porosity including the patchy porosity pattern and average size of high porosity patches with some similarity to the pattern from the Widuri field analogue (Figure 8.33).

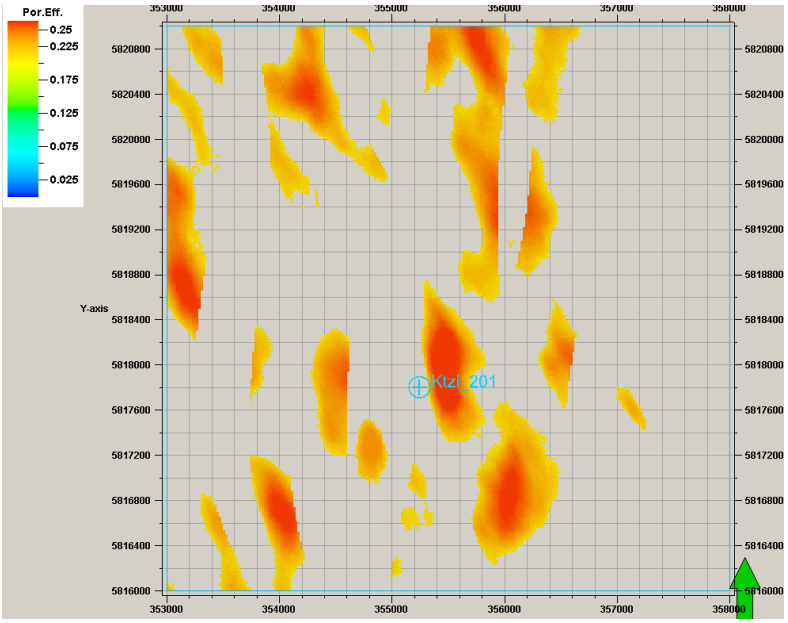

Figure 8.33 Effective porosity (selected interval 0.21 to 0.27) in layer 14 in the Ketzin model.

The permeability modelling was calibrated to core analyses and was established as a functional relation to the total porosity derived from the well log interpretation. The final geo-model supplied the porosity, permeability and facies designation to the reservoir model used for dynamic flow simulation. The effective porosity was transferred, as the flow simulation will work with the mobile water fraction only. The modelled permeability (Figure 8.34) was transferred as the x-direction permeability to the flow simulation, where permeability anisotropy can be implemented.

An early decision in the project on limiting the study to only one single realisation of the chosen scenario has to some extent handicapped the development of a suitable workflow for the combination of modelling/simulation/monitoring. Future work has to engage in this development and device a scheme for building alternative scenarios to have a range of different models available for the analysis of reservoir response.

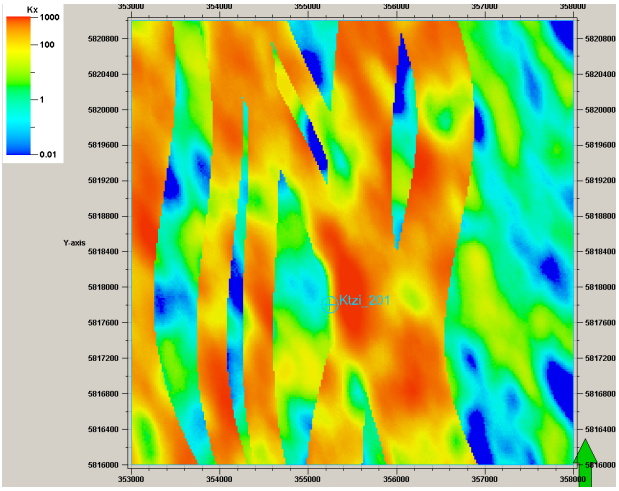

Figure 8.34 Layer 14 in static model v.3.0 showing permeability variability both in the channel belts and the floodplain facies.

8.4.2 Dynamic modelling of injection and predictions

For most of the CO_2 injection simulations the ECLIPSE100 reservoir simulation program (Schlumberger GeoQuest, 2006) is used. To enable a realistic simulation of the solubility conditions, the simulator oil and gas phases are used to represent the water and CO_2, respectively. The phase behaviour is described by black-oil PVT tables (Chang et al., 1998), keeping in mind that ECLIPSE100 is isothermal.

The modelling of the reservoir was carried out in tight cooperation between GFZ, University of Stuttgart and GEUS. The first flow simulations were performed by GEUS based on discussions with University of Stuttgart and Shell International. These initial simulations supplied the first illustration of the distribution of CO_2 during an injection scenario, and proved very useful in the process of communication and for the material needed for obtaining permissions for the CO_2 operation. For the updated model, later simulations of the distribution after 60.000 tons of injected CO_2, showed approximately the same pattern although reaching slightly further into the reservoir. A comparison of the distribution pattern is shown in Figure 8.35 and Figure 8.36.

When comparing the different simulations it must be noted that several different input parameters have uncertainty attached, and all have an influence on the amount of gas-phase CO_2 available for the plume propagation.

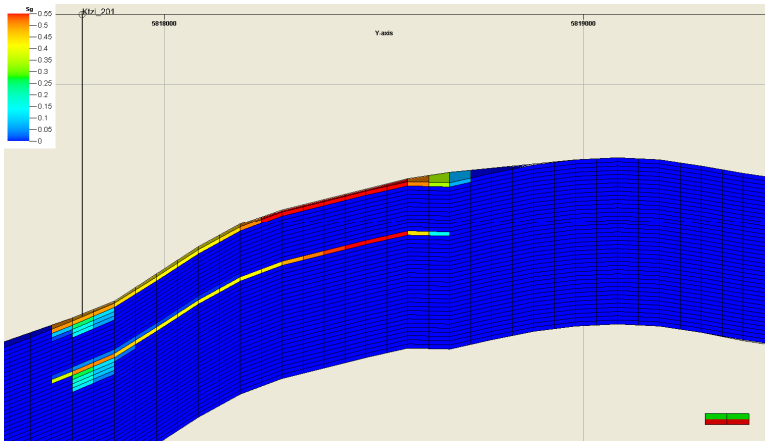

Figure 8.35 N-S section in the Stuttgart Formation in the Ketzin reservoir model v.0.1 with CO_2 saturation after 2.5 years injection of the amount of 60.000 tons. The CO_2 is filling into two high-permeability layers and extending up to 1 km away from the injection well. (Frykman, 2009b).

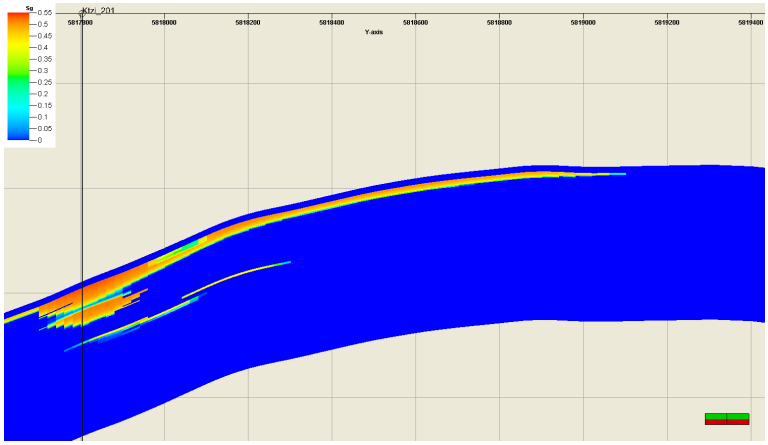

Figure 8.36 N-S section in the Stuttgart Formation in the Ketzin reservoir model v.4.0 with CO_2 saturation after injection of the amount of 60,000 tons.

8.5 Verification: Integration of PA and monitoring

8.5.1 Comparison of predictions and monitoring observations

The first exercise in performance assessment in the project was instituted as a competition for the modelling groups to give their independent predictions of the arrival times for the CO_2 at the two observation wells. Besides the entertainment, this exercise proved very useful later in the overall discussions on how to structure a sensible PA.

One of the first more direct observations of the reservoir behaviour was when the arrival of CO_2 was recorded at the first observation well Ktzi 200, being located 50 m east of the injection well Ktzi 201. CO_2 arrival was defined as the arrival of gaseous CO_2 in the observation well Ktzi 200 due to the fact, that CO_2 was measured as such with the gas membrane sensor) (Zimmer et al., 2011b). The sensor was deployed in the observation well at a level much above the reservoir layer, and therefore the location of the entry in the

observation well of the CO_2 is not known. The arrival time was well predicted by flow models (see example in Figure 8.37), which supports that the permeability connection between the two wells is fairly continuous (Kempka et al., 2010).

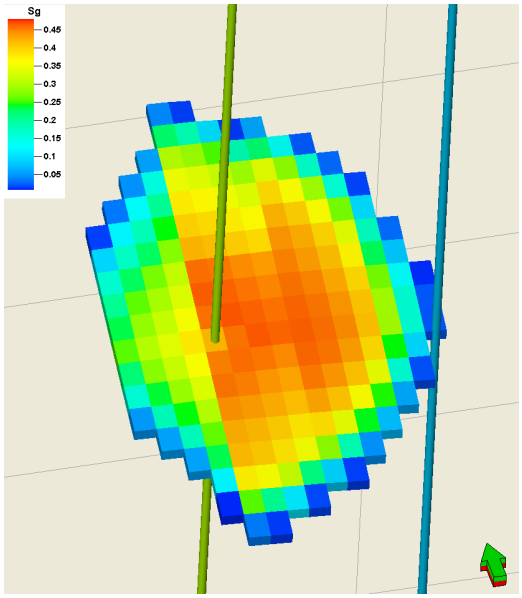

Figure 8.37 Oblique map view of the CO_2 plume in the simulation of arrival time from the injection well Ktzi 201 (at left) to the observation well Ktzi 200 (at right).

The prediction of arrival time has been carried out by applying different numerical simulation codes: as e.g. ECLIPSE 100 (E100, black-oil simulator), ECLIPSE 300 (E300, compositional CO_2STORE) and MUFTE-UG (Multiphase Flow, Transport and Energy model with unstructured grid). The numerical codes were used for the predictive modelling applying the real injection rates, and the geological model applied has been the same for all simulations. The computational results depicted in Figure 8.38 show a relatively good agreement with the data measured at the first observation well Ktzi 200 by the gas membrane sensor. The mismatch between simulated and measured arrival times ranges between 8% and 18% (Frykman et al., 2010; Kempka et al., 2010).

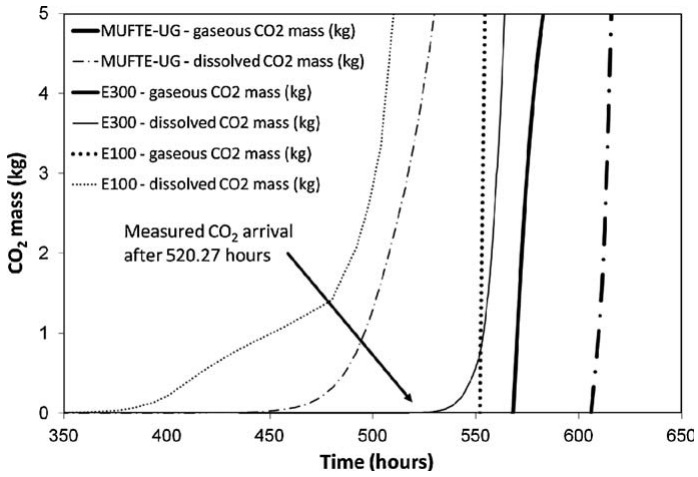

Figure 8.38 CO_2 arrival times at Ktzi 200 as predicted by the different simulators (Kempka et al., 2010).

The simulations could not fit the arrival time at the second observation well Ktzi 202 (located 112 m away from the injection well Ktzi 201), which exceeded the calculated ones by a factor of about 3. Therefore, further research regarding the model improvement was focused on the implementation of heterogeneities, and also on the sensitivity of input parameters regarding changes (Frykman et al., 2010). The significant delay indicates that some sort of flow barrier could exist between the injection and the observation well. The heterogeneity in the fluvial system which is interpreted to represent the Ketzin setting certainly allows for short-scale variations in flow properties, although the exact nature and geometry of a low permeability body at that location is uncertain.
As mentioned, most of the work has related to a single realisation out of the multiple that could have been built from the same input, and also based on the concept for one single scenario for the depositional system. This therefore limits the general conclusions on the success of matching simulations with monitoring data.

For the Ketzin site and its multi-disciplinary monitoring program it was concluded that a more comprehensive phase of data integration and data matching has to be scheduled. Beyond the FP6 research projects CO_2SINK and CO_2ReMoVe, the national funded project CO_2MAN is now continuing with processing and interpretation of the gathered field results, in combination with modelling predictions. There was a strong demand to investigate intensively the reasons for the late arrival time at the Ktzi 202 in comparison to the estimates by the model calculations. It has been deduced that efficient history matching requires an integrated iterative modelling framework. Therefore, extensive integration of new data (seismic, geoelectric, well logging) was undertaken for revision of the static model. The new data lead to an updated facies model with revised poro-perm relationship of the Stuttgart formation, and after incorporating also other influential changes, consequently an agreement of the Ketzin reservoir model was obtained with the two observed CO_2 arrival times (Kempka et al., 2011). Conclusions and publications regarding this matching work are still in process within the project CO_2MAN.

8.5.2 Evaluation of comparisons

At the Ketzin site the CO_2 signature has been detected and recorded, by raw data inspection and by time-lapse results of various monitoring tools. Most of the methods are used for detection of CO_2 only. Currently, the quantitative analysis of the CO_2 plume volume in the reservoir as part of the monitoring and verification program is still ongoing. First promising estimates have been derived from the time-lapse result of the 3D seismic repeat by implementing results from PNG well logging and petrophysical measurements on core samples as additional assets to derive the total amount of CO_2 from the seismic data in Ivanova et al. (2012). The slight underestimation in comparision with the actual amount of CO_2 injected is due to the remaining uncertainties by the number of parameters deployed. because they offered. A similar workflow is intended to be applied for the ERT data sets as alternative approach to contribute independently to this quantification task.

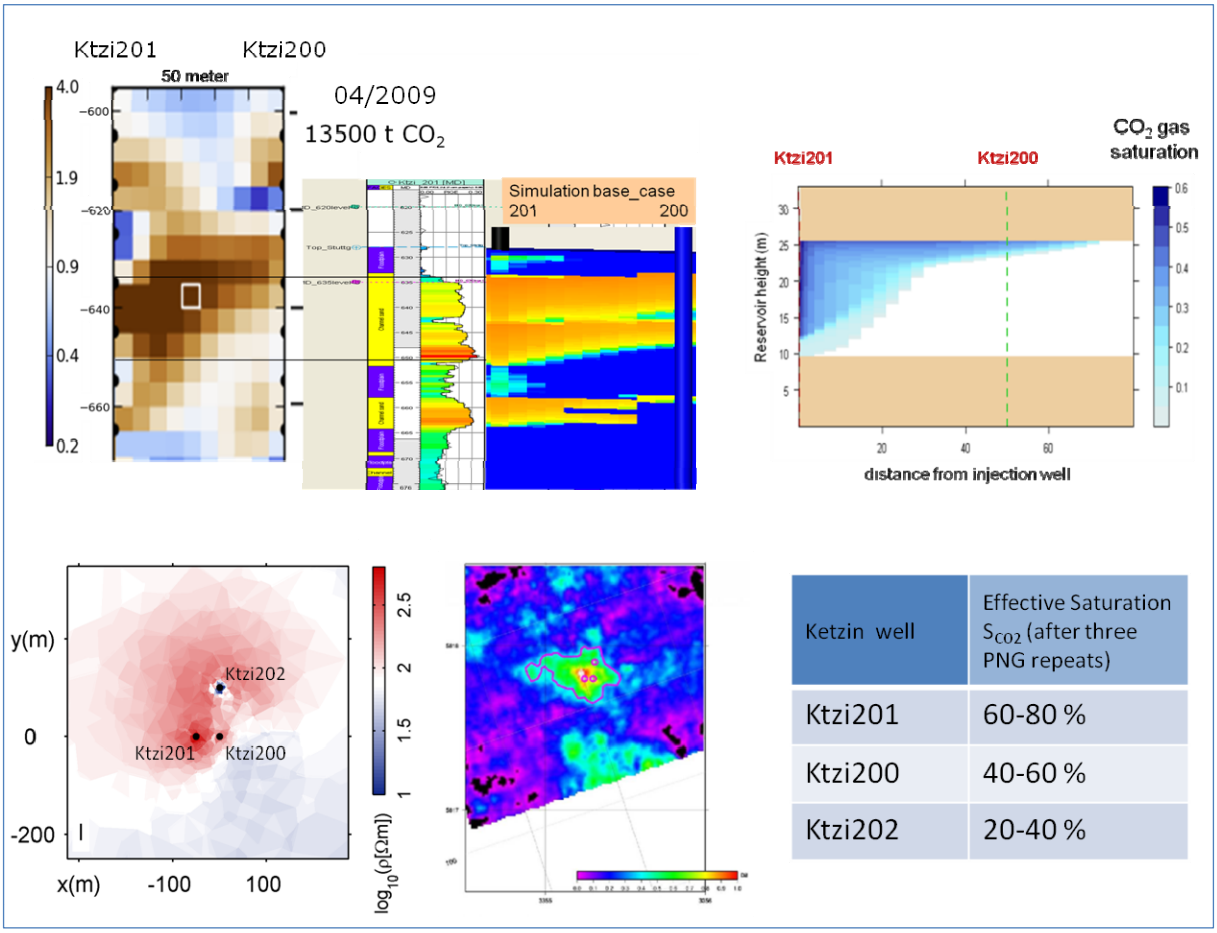

Figure 8.39 2D crosshole resistivity profile (Schmidt-Hattenberger et al., 2011) was visually matched with porosity log and 2D reservoir model realizations performed with ECLIPSE (Frykman, 2009b) and TOUGH2 (Lengler et al., 2010). The results are in good agreement with results from a large-scale geoelectric survey (Bergmann et al., 2012) and the 3D seismic repeat (Juhlin et al., 2010), both have been correlated with the near-wellbore results from gas saturation measurements (PNG logging), simplified from table 4 of Ivanova et al. (2012).

When combining monitoring data with modelling results, it is critical to be aware of the scale and the volume which we are informed about (Figure 8.39). Small scale observations in a local area, however accurate and precise, cannot inform much about any larger scales, and a large scale observation of a response from a large volume cannot inform about heterogeneity at smaller scale (Frykman 2009c). This enigma is also a challenge.
For the Ketzin site there is a unique opportunity of multiple data sets originating at different scales and being independent. The integration of these, and the ability to model the system response in parallel with analysing the monitoring data, will result in a better understanding of the performance of geological systems when they are subjected to injection of CO_2 at an industrial scale. However, the leap to industrial scale CO_2 injection could very well modify the evaluation criteria developed from a relatively small pilot site. Some of the details described in the Ketzin study might not be discernable at industrial scale injection sites (1000 kT/year plus).

8.6 Conclusions and Outlook

General Outcome
The monitoring concept at Ketzin is compliant with national regulations, notably the Mining law used for seasonal gas storage and transport and with the Environmental law, which covers dangerous surface industrial facilities, and "classified installations". The latter includes the EU Water Directive. The mining authority issued the permission for operating the test site.
Based on the intense and complex monitoring program one can conclude that no safety issues were encountered until now, nor is there any indication that issues will occur in the future.

Innovative tools
The technology of electrical resistivity tomography (ERT) downhole installation has been successfully site-proofed, and the permanent vertical electrode system performs as a valuable interface for CSEM/MT measurements. For the conditions at the Ketzin site, seismic is the preferred method for structural imaging, and geoelectric for imaging pore fluid changes. To exploit the advantages of both methods, we address current work on the incorporation of structural seismic information as a priori constraints in the ERT inversion.

Passive seismic receivers (here as downhole instruments and broadband stations) should be installed from the very beginning of a storage experiment, i.e. starting with a baseline from the pre-injection time. An interesting option in the near future could be the application of 3C-geophones carried out as behind casing tools, preferably as fibre-optic design.

Overall, there is no tool at Ketzin which is useless or which cannot be recommended. However, after finishing the active CO_2 injection period one should rank the tools after a priority list. For example, the passive seismic surface monitoring is currently in an experimental stage and will not have highest priority for CO_2 detection at Ketzin.

Constraints
Financial constraints did pose a limit to the monitoring. For instance, the number of seismic repeats and of logging campaigns is limited. The original microseismic part of CO_2SINK was cancelled because budget was lacking. In scheduling the monitoring concept, some costs were underestimated, as e.g. the need for a lubricator system at both pressurized observation wells during all downhole seismic campaigns after the breakthrough of CO_2.

Outreach
There is a strong interest in extrapolation of results to other sites, e.g. one could intensify a direct comparison of data and experiences between Nagaoka site (Japan) and Cranfield/Mississippi site (USA), which operate at the pilot scale. This will help to broaden knowledge, and to conclude on some general, resilient recommendations which could be helpful for future storage sites.

At this stage, a number of generic conclusions can be drawn. The deployment of smart-casing technology is very promising, as well as combined measurements (e.g. surface-downhole / multi-parameter / multiple scales). This helps to enlarge and to better verify the observation area of plume migration and provides more confidence in the measurements. Furthermore, the development of optimal adapted technology for detection is worthwhile, as e.g. the gas membrane sensor - GMS, and the buried seismic sensors in the field – the so-called TNO array. The critical evaluation of the deployed monitoring tools will provide a true contribution to the operational reservoir management, and to the performance and risk assessment.

References:

Arts, R., Meekes, J., Brouwer, J., van der Werf, M., Noorlandt, R., Paap, B., Visser, W., Vandeweijer, V., Lüth, S., Giese, R., Maas, J., 2011. Results of a monitoring pilot with a permanent buried multicomponent seismic array at Ketzin. Energy Procedia 4, 3588-3595.

Bergmann, P., Lengler, U., Schmidt-Hattenberger, C., Giese, R., Norden, B., 2010. Modelling the geoelectric and seismic reservoir response caused by carbon dioxide injection based on multiphase flow simulation: Results from the CO_2SINK project. Chemie der Erde 70 (S3), 173-183.

Bergmann, P., Yang, C., Lüth, S., Juhlin, C., Cosma, C., 2011. Time-lapse processing of 2D seismic profiles with testing of static correction methods at the CO_2 injection site Ketzin (Germany). Journal of Applied Geophysics 75 (1), 124-139.

Bergmann, P., Schmidt-Hattenberger, C., Kiessling, D., Rücker, C., Labitzke, T., Henninges, J., Baumann, G., Schütt, H., 2012. Surface-Downhole Electrical Resistivity Tomography applied to Monitoring of the CO2 Storage Ketzin (Germany). Geophysics 77 (6), B253-B267.

Bourgeois, B. and Girard, J-F, 2010. First modelling results of the EM response of a CO2 storage in the Paris basin. Oil & Gas Science and Technology - Rev. IFP 2010; 65(4): 597-614.

Bridge, J.S. and Leeder, M.R. 1979: A simulation model of alluvial stratigraphy. Sedimentology 26, 617-644.

Bridge, J. S., and S. D. Mackey, 1993, A theoretical study of fluvial sandstone body dimensions, in S. S. Flint and I. D. Bryant, eds., Geological modeling of hydrocarbon reservoirs: International Association of Sedimentologists, Special Publication 15, Utrecht, Netherlands, 213–236.

Carter, D.C. 2003: 3-D seismic geomorphology: Insights into fluvial reservoir deposition and performance, Widuri field, Java Sea AAPG Bulletin, v. 87, no. 6 (June 2003), 909–934.

Cosma, C., and Enescu, N., 2011. CO_2 Injection Monitoring by High Resolution Time-lapse Crosshole Seismics (The CO_2SINK Team - CO_2SINK Project), 1st Sustainable Earth Sciences Conference & Exhibition – Technologies for Sustainable Use of the Deep Sub-surface, 8-11 November 2011, Valencia, Spain, EarthDoc-55587.

CO_2SINK Project Team, 2005, CO2SINK - The first year, Greenhouse Issues, no. 79, September 2005, p. 11-13, http://www.ieaghg.org/index.php?/2009120762/greenhouse-issues-september-2005-number-79.html#article16

Delatre, M., Manceau, J.C., Bitri, A., 2011, Preliminary results for broadband seismic noise correlation for CO_2 reservoir monitoring : the Ketzin test case. EAGE Third Passive Seismic Workshop – Actively Passive! , 27-30 March 2011, Athens, Greece, EarthDoc-49410.

Freifeld, B. M., Daley, T. M., Hovorka, S. D., Henninges, J., Underschultz, J., Sharma, S., 2009, Recent advances in well-based monitoring of CO_2 sequestration. Energy Procedia 1, 2277-2284.
Götz, J., Giese, R., Lüth, S., Schmidt-Hattenberger, C., Juhlin, C., Cosma, C., 2011a. Borehole seismic monitoring of CO_2 storage within a saline aquifer at Ketzin, Germany. EAGE Borehole Geophysics Workshop - Emphasis on 3D VSP, 16-19 January 2011, Istanbul, Turkey, EarthDoc-47183.

Götz, J., 2011b. CO_2ReMoVe Internal Report 'Deliverable D3.8.3C_VSP and MSP Final Report'.

Götz, J., 2012. Borehole seismic monitoring of CO_2 storage within a saline aquifer at Ketzin, Germany. Ph.D. thesis (in prep.). Now finished and online published under: Technische Universität Berlin, http://opus4.kobv.de/opus4-tuberlin/frontdoor/index/index/docId/4630

Förster, A., Norden, B., Zinck-Jørgensen, K., Frykmann, P., Kulenkampf, J., Spangenberg, E., Erzinger, J., Zimmer, M., Kopp, J., Borm, G., Juhlin, C., Cosma, C., Hurter, S., 2006. Baseline characterization of the CO_2SINK geological storage site at Ketzin, Germany. Environmental Geosciences 13 (3), 145-161.

Förster, A., Giese, R., Juhlin, C., Norden, B., Springer, N., CO_2SINK-Group, 2009. The Geology of the CO_2SINK Site: From Regional Scale to Laboratory Scale. Energy Procedia 1, 2911-2918.

Förster, A., Schöner, R., Förster, H.-J., Norden, B., Blaschke, A.-W., Luckert, J., Beutler, G., Gaupp, R., & Rhede, D., 2010. Reservoir characterization of a CO_2 storage aquifer: The Upper Triassic Stuttgart Formation in the Northeast German Basin. Marine and Petroleum Geology 27, 2156-2172.

Flach, T., Garnett, A., Carpenter, M., 2008, Safety Case for Long Term Storage Containment, CO_2Sink In-situ R&D Laboratory for Geological Storage of CO2, CO_2SINK Report No.: D4.1-4, Revision 06, 24 April 2008.

Freifeld, B.M., Daley, T.M., Hovorka, S.D., Henninges, J., Underschultz, J., Sharma, S., 2009. Recent advances in well-based monitoring of CO_2 sequestration. Energy Procedia 1, 2277-2284.

Frykman, P., 2009a. CO_2ReMoVe Internal Report. Deliverable D2.6.1A Performance Assessment part A: Background and Setting of the Ketzin Site (version 01).

Frykman, P., 2009b. CO_2ReMoVe Internal Report. Deliverable D2.6.1B Performance assessment part B: Medium time-scale plume development simulated in the Ketzin site model v. 0.0 (version 02).

Frykman, P., 2009c. CO_2ReMoVe Internal Report. Deliverable D2.6.1C Performance assessment part C: Comparison of geoelectric surface-downhole monitoring observations and simulated prediction of CO_2 plume extent (version 01).

Frykman, P., Class, H., Kempka, T., 2010. Chapter 4: Dynamic Flow Modelling, CO_2SINK Summary Technical Report, http://cordis.europa.eu/documents/documentlibrary/123655671EN6.pdf

Girard, J.-F., Bourgeois, B., Rohmer, J., Schmidt-Hattenberger, C., 2009. The LEMAM array for CO_2 injection monitoring : modelling results and baseline at Ketzin in August 2008. EGU General Assembly - 19-24 April 2009, Vienna, Austria.

Girard, J.-F., Coppo, N., Rohmer, J., Bourgeois, B., Naudet, V., & Schmidt-Hattenberger, C., 2011. Time-lapse CSEM monitoring of the Ketzin (Germany) CO_2 injection using 2xMAM configuration. Energy Procedia 4, 3322-3329.

Henninges, J., Kopp, A., Le Bastard, E., Brandt, W., 2009. Thermal effects during CO_2 injection and well cementing at Ketzin. EGU General Assembly 2009, Vienna (Austria). Geophysical Research Abstracts 11, EGU2009-11412-1.

Henninges, J., Baumann, G., Freifeld, B. M., 2011a. Near-wellbore characterization of CO_2 migration at Ketzin using PNG and DTS measurements. IEAGHG 7th Monitoring Network Meeting (Potsdam 2011, Germany). Presentation.
http://www.ieaghg.org/docs/General_Docs/7_Mon/0303_2011-06_IEAGHG-Monitoring-Network-Henninges_web_SECURED.pdf

Henninges, J., Liebscher, A., Bannach, A., Brandt, W., Hurter, S., Köhler, S., Möller, F., CO_2SINK-Group, 2011b. P-T-ρ and two-phase fluid conditions with inverted density profile in observation wells at the CO_2 storage site at Ketzin (Germany). Energy Procedia 4, 6085-6090.

Ivandic, M., Yang, C., Lüth, S., Cosma, C., Juhlin, C., 2012. Time-lapse analysis of sparse 3D seismic data from the CO_2 storage pilot site at Ketzin, Germany. Journal of Applied Geophysics 84, 14 – 28.

Ivanova A., A. Kashubin, N. Juhonjuntti, J. Kummerow, J. Henninges, Ch. Juhlin, and S. Lüth, 2012. 4D seismic data analysis at Ketzin, Germany, and CO_2 volumetric estimation using petrophysical data, core measurements and well logging: a case study, Geophysical Prospecting 60, 957–973.

Juhlin, C., Giese, R., Zinck-Jørgensen, K., Cosma, C., Kazemeini, H., Juhojuntti, N., Lüth, S., Norden, B., Förster, A., 2007. Case History: 3D baseline seismics at Ketzin, Germany: The CO_2SINK project. Geophysics 72 (5), B121-B132.

Juhlin, C., Bergmann, P., Giese, R., Götz, J., Ivanova, A., Juhojuntti, N., Kashubin, A., Lüth, S., Yang, C., Zhang, F., 2010, Preliminary Results from a Repeat 3D Seismic Survey at the CO_2SINK Injection Site, Ketzin, Germany. 72nd EAGE Conference & Exhibition incorporating SPE EUROPEC 2010, Barcelona, Spain, 14 - 17 June 2010, EarthDoc-39731-1.

Kazemeini, S., Juhlin, C., Zinck-Jørgensen, K., Norden, B., 2009. Application of the continuous wavelet transform on seismic data for mapping of channel deposits and gas detection at the CO_2SINK site, Ketzin, Germany. Geophysical Prospecting 57, 111-123.

Kempka, T., Kühn, M., Class, H., Frykman, P., Kopp, A., Nielsen, C.M., Probst, P., 2010, Modelling of CO_2 arrival time at Ketzin - Part I. International Journal of Greenhouse Gas Control 4 (6), 1007-1015.

Kempka, Th. et al., (2011). 7th Monitoring Network Meeting, Potsdam, Germany. Presentation.
http://www.ieaghg.org/docs/General_Docs/7_Mon/0306_Kempka_et_al-IEAGHG_Monitoring_2011_WEB_SECURED.pdf

Kiessling, D., Schmidt-Hattenberger, C., Schütt, H., Schilling, F., Krüger, K., Schöbel, B., Danckwardt, E., Kummerow, J., CO_2SINK-Group, 2010. Geoelectrical methods for monitoring geological CO_2 storage: First results from cross-hole and surface-downhole measurements from the CO_2SINK test site at Ketzin (Germany). International Journal of Greenhouse Gas Control 4 (5), 816-826.

Liebscher, A., Martens, S., Möller, F. & Kühn, M., 2012. On-shore CO_2 storage in Germany – experiences gained from the Ketzin pilot site, Brandenburg, the sole German national CO_2 storage project. In: Gluyas, J. & Mathias, S. (eds.) Geoscience of carbon dioxide (CO_2) storage. Woodhead Publishing Limited, ISBN 9780857094278.

Lengler, U., M. de Lucia, M. Kühn, 2010. The impact of heterogeneity on the distribution of CO_2: Numerical simulation of CO_2 storage at Ketzin. International Journal of Greenhouse Gas Control, 4 (6), 1016-1025.

Lüth, S., Bergmann, P., Cosma, C., Enescu, N., Giese, R., Götz, J., Ivanova, A., Juhlin, C., Kashubin, A., Yang, C., Zhang, F., 2011. Time-lapse seismic surface and down-hole measurements for monitoring CO_2 storage in the CO_2SINK project (Ketzin, Germany). Energy Procedia 4, 3435-3442.

Miall, A.D. (2006) Reconstructing the architecture and sequence stratigraphy of the preserved fluvial record as a tool for reservoir development: A reality check, Am. Assoc. Petrol. Geol. Bull. 90, 7, 989-1002.

Morozova, D., Wandrey, M., Alawi, M., Zimmer, M., Vieth, A., Zettlitzer, M., Würdemann, H., 2010. Monitoring of the microbial community composition in saline aquifers during CO_2 storage by fluorescence in situ hybridisation. International Journal of Greenhouse Gas Control 4 (6), 981-989.

Morozova, D., Zettlitzer, M., Let, D., Würdemann, H., and the CO_2SINK Group, 2011. Monitoring of the microbial community composition in deep subsurface saline aquifers during CO_2 storage in Ketzin, Germany. Energy Procedia 4, 4362–4370.

Norden, B., Förster, A., Vu-Hoang, D., Marcelis, F., Springer, N., Nir, I. L., 2010. Lithological and Petrophysical Core-Log Interpretation in CO_2SINK, the European CO_2 Onshore Research Storage and Verification Project. SPE Res Eval & Eng 13 (2), 179-192.

Norden, B., 2011. Modelling of the near-surface groundwater flow system at the CO_2SINK site Ketzin, Germany. Z. dt. Ges. Geowiss. 162/1, 63-77.

Overton, G., 2011. Photonics Applied: Optical Sensing: Downhole sensing puts fiber optics to the test. Laser Focus World, http://www.laserfocusworld.com/articles/2011/04/photonics-applied-optical-sensing-downhole-sensing-puts-fiber-optics-to-the-test.html

Rossi, G., 2011. CO_2ReMoVe Internal Report. Deliverable_D3.8.1C.pdf.
Schilling, F., Borm, G., Würdemann, H., Möller, F., Kühn, M., CO_2SINK-Group, 2009. Status Report on the First European on-shore CO_2 Storage Site at Ketzin (Germany). Energy Procedia 1, 2029-2035.

Schmidt-Hattenberger, C., Moeller, F., Liebscher, A., Koehler, S.,2009. Permanent downhole fiber optic pressure and temperature monitoring during CO_2 injection. EGU General Assembly 2009, Vienna (Austria). Geophysical Research Abstracts 11, EGU2009-11513.

Schmidt-Hattenberger, C., Bergmann, P., Kießling, D., Krüger, K., Rücker, C., Schütt, H., Ketzin-Group, 2011. Application of a Vertical Electrical Resistivity Array (VERA) for monitoring CO_2 migration at the Ketzin site: First performance evaluation. Energy Procedia 4, 3363-3370.

Streich, R., M. Becken, U. Matzander, and O. Ritter, 2011. Strategies for land-based controlled-source electromagnetic surveying in high-noise regions: The Leading Edge, 30, 1174-1181.

Wandrey, M., Fischer, S., Zemke K., Liebscher A., Scherf, A.-K., Vieth-Hillebrand, A., Zettlitzer, M., Würdemann, H., 2011. Monitoring petrophysical, mineralogical, geochemical and

microbiological effects of CO_2 exposure - Results of long-term experiments under in situ condition. Energy Procedia, 4, 3644–3650.

Wiese, B., Böhner, J., Enachescu, C., Würdemann, H., Zimmermann, G., 2010. Hydraulic characterisation of the Stuttgart formation at the pilot test site for CO_2 storage, Ketzin, Germany. International Journal of Greenhouse Gas Control Volume 4, 960-971.

Wiese, B., Otto, C., Möller, F., Kühn, M., Schmidt-Hattenberger, C. 2011. Heat production in the injection borehole at the pilot test site for CO_2 storage, Ketzin, Germany, ModelCare 2011: The 8th International Conference on Calibration and Reliability in Groundwater Modeling, Leipzig, 18-22 September 2011,
http://www.modelcare2011.org/MODELCARE_2011/Start_files/MC_Abstractband_web.pdf

Würdemann, H., Möller, F., Kühn, M., Heidug, W., Christensen, N., Borm, G., Schilling, F., CO_2SINK-Group, 2010. CO_2SINK - From site characterisation and risk assessment to monitoring and verification: One year of operational experience with the field laboratory for CO_2 storage at Ketzin, Germany. International Journal of Greenhouse Gas Control 4, 938-951.

Yang, C., Juhlin, C., Enescu, N., Cosma, C., Lüth, S., 2010. Moving source profile data processing, modelling and comparison with 3D surface seismic data at the CO_2SINK project site, Ketzin, Germany. Near Surface Geophysics 8, 601-610.

Zettlitzer, M., Moeller, F., Morozova, D., Lokay, P., Würdemann, H., and the CO_2SINK Group, 2010. Re-establishment of proper injectivity of the CO_2-injection well Ketzin-201. International Journal of Greenhouse Gas Control 4, 952-959.

Zimmer, M., Erzinger, J., Kujawa, C., CO_2SINK-Group. 2011a. The gas membrane sensor (GMS): A new method for gas measurements in deep boreholes applied at the CO_2SINK site. International Journal of Greenhouse Gas Control 5, 995-1001.

Zimmer, M., Pilz, P., Erzinger, J., 2011b. Long-term surface carbon dioxide flux monitoring at the Ketzin carbon dioxide storage test site. Environmental Geosciences 18 (2), 119-130.